# ANALYSIS OF PAVEMENTS UNDER THERMAL AND VEHICLE LOADS USING SHEAR DEFORMATION PLATE THEORY

# PROJECT


*By*

**Ravi Shankar**

**19CE01033**




**SCHOOL OF INFRASTRUCTURE**
**INDIAN INSTITUTE OF TECHNOLOGY BHUBANESWAR**
**BHUBANESWAR -752050, ODISHA**


**MAY 2023**

# CONTENTS

# LIST OF FIGURES

# LIST OF TABLES

# NOTATIONS

a and b: rectangular plate dimensions

h: Plate thickness

E: Young's modulus

D: Flexural rigidity

P: Distributed load intensity

w: Deflection

G: Shear modulus

$\mu$ : Poisson's ratio

Q: Shear force

C: Shear stiffness

$\phi$ : Potential function

$\psi$ : Stream function

$\tau$: Shear stress

$\sigma$: Normal stress

$\gamma$ : Shear strain

$\varepsilon$: Normal strain

# Chapter 1
# INTRODUCTION

## 1.1 General

Roads are critical public infrastructure since they constitute an essential requirement for any country's social and economic development. Roads require preservation, maintenance, repair, and rehabilitation. Reliable information about the state of road preservation is required in order to plan and carry out these actions. The challenging aspect of road assessment lies in its structural state.

A pavement is a layered structure made up of different materials such as cement concrete, bound or unbound stone aggregates, asphaltic material, and more. The mechanical behaviour of these materials is intricate and influenced by changes in temperature, time, or stress. As a result, it is difficult to comprehend the performance of a pavement structure when subjected to moving loads of vehicles and changing climatic conditions. Additionally, the layers of various materials used in pavements can vary in thickness, making pavement analysis complex due to deformation caused by changes in moisture content and temperature resulting in internal stresses. Because of these factors, the analysis of pavement structures is challenging and requires expertise in material characterization, mathematics, and modelling.

There has been a strong push to refine our understanding of how pavements react to varying loads by creating more sophisticated modelling and analysis approaches. The Shear Deformation Plate Theory (SDPT) is one such method, and it has become increasingly popular due to its ability to accurately predict the shear deformation affects that occur in thin plates when subjected to bending loads.

The SDPT approach models the plate as a stack of thin layers with varying orientations and takes shear deformation at each layer into consideration. Because of their thin and flat form, pavements are ideal candidates for this method of analysis since it provides a more realistic picture of the stress and strain distribution within the plate.

In this project, we aim to apply the SDPT method to analyse the behaviour of pavements under thermal and vehicle loads. Cracking and other damage can occur as a result of thermal variations causing the pavement to expand and contract, and vehicle loads

can induce deformation and stress in the pavement. We can learn more about how pavements react under certain loading conditions and pinpoint possible weak spots by employing the SDPT technique.

In a pavement construction, the loading conditions have a major impact on how the various layers behave. The top layer of asphalt or concrete pavement is what bears the brunt of a vehicle's weight as it travels over the surface. This leads to layer deformation and stress, which can cause damage like cracking and rutting. Extreme expansion or contraction of the pavement layer may occur under thermal loading circumstances. This can lead to the pavement warping and cracking, which in turn can weaken the pavement even more.

The subgrade layer, found beneath the top layer, is likewise impacted by traffic and temperature. A vehicle's weight is transferred through the pavement's top layer and into the subgrade underneath. This can lead to settlement and other forms of damage by deforming and stressing the subgrade layer. Temperature-induced volume changes can occur in the subgrade layer under thermal loading circumstances. This can result in heave or settlement, as the soil either expands or contracts.

Both vehicular and thermal stresses can be felt by the base layer, which sits beneath the surface and above the subgrade. The base layer acts as a structural support system for the pavement and spreads the weight of the top layer over a broader region.

In conclusion, vehicular and thermal stresses affect all layers of a pavement structure, but each layer reacts differently to these loads. For planning and maintaining long-lasting and secure pavement systems, knowledge of the behaviour of each layer under varying loading situations is essential.

A pavement is composed of layers that are horizontally stacked, including compacted soil, unbound granular material like stone aggregates, asphalt mix, cement concrete, or other bound materials. Figure 1.1 displays a standard cross-section of an asphalt and concrete pavement, with concrete pavements often featuring joints while asphalt pavements typically do not. Concrete pavements consist of concrete slabs with finite dimensions connected to adjacent slabs using steel bars. Dowel bars are placed along transverse joints, and tie bars are located along longitudinal joints (see Figure 1.2). On the other hand, block pavements or segmental pavements consist of interlocking cement concrete blocks, and their structural behaviour is different from conventional asphalt or concrete pavements.

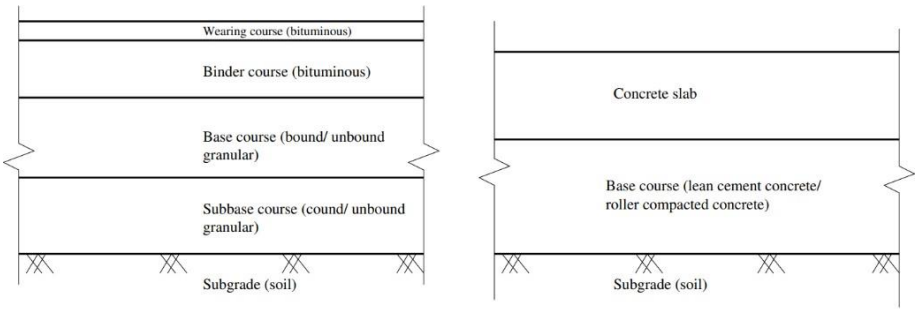


(a) An asphalt pavement section (b) A concrete pavement section

Figure 1: Typical cross-section of an asphalt and a concrete pavement.

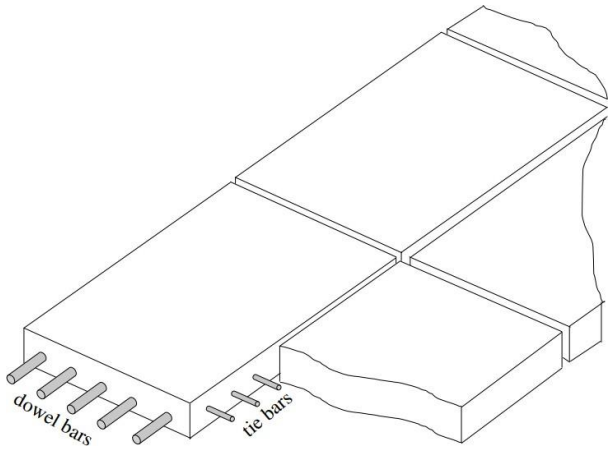


Figure 2: Dowel bar and tie bar arrangement in concrete pavement.

## 1.2 Sign conventions

Some of the fundamental and frequently used equations, which are also mentioned and used in this report. There is also some use of soil mechanics concepts.

The sign convention followed in the present book is shown in Figure 1.3 for the Cartesian coordinate system.

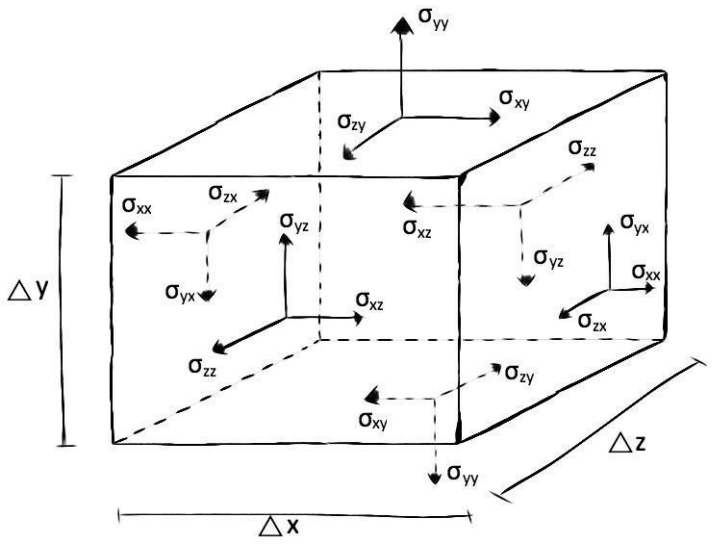


Figure 1.3: Sign convention in the Cartesian system followed.

## 1.3 Objective

The objective of this study is to analyse the behaviour of pavement under vehicle and thermal stresses by employing the first-order shear deformation plate theory. The theory allows for precise prediction of stresses and deformations inside the pavement structure, which aids in gaining insight into the pavement's overall performance.

The effect of temperature changes on the pavement structure will be investigated, as will the pavement's behaviour under static stresses. In order to forecast the stress and deformation responses of the pavement, the analysis will make use of numerical simulation technologies such finite element analysis.

This research aims to shed light on how pavement reacts to various loads and to reveal any design or material flaws that may compromise the pavement's performance. Engineers and planners can use the results of this study to better develop and maintain sustainable pavement systems that can resist a wide variety of loading scenarios.

## 1.4 Scope

The aim of this discussion is to present a conceptual framework for understanding the fundamental principles of load and thermal stresses in pavements. As a pavement is continually subjected to traffic loading and temperature variations while in use, analyzing

its structure helps predict or explain its response to load based on physical principles, which can be verified through experimental observations. This, in turn, increases confidence in the design, evaluation, and maintenance planning of road infrastructure.

Concrete pavements are often idealized as a plate resting on an elastic foundation, with the assumption that the load is transferred through bending and the slab thickness remains unchanged under load.

Since pavements are multi-layered structures, obtaining a closed-form solution of their response to load is typically challenging. For design purposes, pavement analysis can be carried out using software like MATLAB, and various codes and guidelines offer ready-to-use analysis charts. However, the algorithms and assumptions involved in the analysis process may not always be apparent to pavement designers who use these software or charts, highlighting the need to understand the assumptions and basic formulations required for analysing a pavement structure. Using methodologies based on finite elements, discovering the interrelationships between the factors that affect the performance of concrete pavements.

In addition, the following objectives of this study are:

- In addition, the purpose is to investigate both the global and local behaviours of pavements when they are being subjected to the loads that were applied.
- To investigate and address the effects that various debonding layers have on concrete pavement
- To gain a better knowledge of the behaviours of pavement under environmental factors so as to respond to these effects.

The study of pavement behaviour under different loading conditions, including vehicle and thermal loads, is a complex and dynamic field with many opportunities for future research. Some of the potential areas for future research in this field include:

1. Building more complex numerical models to replicate how pavements react to various loads. To better reflect how pavements actually behave in the real world, it may be necessary to include other elements such as wetness, ageing, and tire-pavement interaction.
2. Looking at how new technology and materials could be used to make pavements last longer and be less taxing on the environment. For instance, researchers may look at novel construction processes that lessen the negative effects of paving on the environment, or they may study smart materials that can adjust to different climates.

3. Validating the findings of numerical simulations and laboratory trials by field research. Gathering information about the performance of pavement structures in real-world conditions and contrasting that with the results of computer models is one approach.

# Chapter 2
# LITERATURE REVIEW

## 2.1 General

The plate theories proposed by Reissner and Mindlin [1–3] are well-known and considered a first order shear deformation theory (FSDT). The displacement field is interpreted as linear variations of midplane displacements, and the shear correction factors impact the link between resultant shear forces and shear strains. This theory is easy to implement and cost-effective to compute.

Other plate theories, such as those proposed by Swaminathan [6], Ferreira [7], and Zenkour [8], take into account the effect of transverse shear deformations and are categorized as higher order shear deformation theories (HSDT). Reddy's hypothesis [9] proposes a straightforward higher-order theory that accounts for transverse shear strains and a parabolic variation of the transverse shear strains throughout the thickness. This theory does not require shear correction coefficients when calculating shear stress.

The study by Mohamed Zidi et al. [10] highlights the use of layered materials in various constructions, where homogeneous elastic laminates are bonded using adhesives. The research investigates the effect of several factors, including transversal shear deformation, plate aspect ratio, side-to-thickness ratio, volume fraction distributions, moisture concentration, and elastic foundation parameters, on the structural response of laminated composite constructions. The study aims to apply the four-variable refined plate theory to analyse the behaviour of plates made of functionally changing materials, which are supported by elastic foundations and subjected to bending. The authors emphasize that the concentration of moisture also plays a significant role in the outcome. The developed methodology and formulation are expected to assist engineers in designing plates with varying degrees of functionality in future studies.

An updated version of the basic first-order shear deformation theory has been proposed by the Hoang Nam Nguyen [11]. In this configuration, the transverse shear strain and shear stress both exhibit a parabolic distribution throughout the width of the plates' thickness, but

they both equal zero at the surfaces of the plates. The author was successful in accomplishing this goal by developing a fresh distribution shape function. The new and improved theory does not necessitate the use of a shear correction factor as a result. The Navier solution is utilised in order to study the static bending as well as the free vibration of advanced composite plates that are simply supported. Author claimed that this theory makes it easier to calculate the deflections and frequencies of plates made of modern composite materials. Comparisons of the deflection, axial stresses, transverse shear stresses, and frequency of the plates produced by the proposed theory with the published results of other theories are made in order to demonstrate the effectiveness as well as the precision of the new theory. These comparisons are made with other theories' published results. In addition, discussions on the consequences of a number of different elements, such as the power-law index, slenderness ratio, and aspect ratio, are held. According to the author, these conversations are beneficial to the process of designing and testing new composite constructions.

Many authors, including HeteHnyi [12], Reissner [1], Filonenko Borodich [13], and Pasternak [14], have proposed two-parameter extensions to the classical Winkler model in an effort to make it more realistic. Their model accounts for the result of shear contact between neighbouring spots in the base. The shear parameter in this model is an undetermined experimental variable. Vlasov and Leont'ev [15] have proposed another arbitrary parameter, with a value between 1 and 2 that depends on the soil composition and the thickness of the soil layer. However, they failed to mention how they arrived at this value. Vallabhan and Daloglu [26] demonstrate how an iterative computational technique for plates may be used to estimate the soil parameter, Kolar and Nemec [16] have created a 3D-FEM model based on a concept by Vlasov and Leont'ev [15] that accounts for the input from the soil medium outside the area of the plate. The elastic springs placed at regular intervals along the plate are used to simulate the effects of the foundation's reaction outside the plate. Recently, helik and Saygun [17] introduced a novel finite element technique that incorporates environmental effects by factoring in the material qualities of the soil. Both the plate itself and the external medium are broken down into smaller components called "plate elements" and "soil finite elements" in their research. Celep [18] examined the rectangular elastic plates supported by a tensionless Winkler base.

Rutting damage is exacerbated by applied traffic loading, especially from slow-moving vehicles. The effects of traffic load and temperature on flexible pavement were studied by Zainab Ahmed Alkaissi [19]. High temperatures on the pavement are a direct result of the

climate's influence and are a major contributor to the deterioration of flexible pavements. Pavement rutting is a major issue due to the increased traffic volume and excessive overloading that caused it. A reasonable analytical method for predicting thermal stress in flexible pavement under dynamic behaviour of asphalt mixture layers was demonstrated by Litao et al. Calculation results considering dynamic behaviour show a clear contrast from those with a static model, as shown by the results produced. Seasonal changes in thermally induced strain in flexible pavement are studied by Biswas et al. [20]. Thermal strain is roughly 1.4-2.0 times larger than in warm season, according to the results of field observations and laboratory tests of asphalt slab.

The finite element method is applied by J.M. Duncan [21], to the analysis of pavement structure-representative systems. Author claimed that after analysis shows that extensional strains in the asphalt concrete are high for this pavement (i.e., when the stiffness of the asphalt bound material is low), the granular material exhibits a very low modulus under the loaded area, and a large proportion of the surface deflection can be attributed to deformations within this material. This is the case when the extensional strains in the asphalt concrete are high because the stiffness of the asphalt bound material is low. When the asphalt layer, on the other hand, is rigid, the majority of the surface deflection is contributed by the subgrade.

The first comprehensive analytical solution of concrete pavement under various loading scenarios was carried out by Westergaard [25]. The curling stress calculations developed by Westergaard [25] were updated by Bradbury, who took into account the concrete slab's finiteness in both horizontal directions. The temperature fluctuated linearly with slab depth, according to Westergaard [25]. However, the main disadvantages of using Westergaard's methods are the intricate geometry and loading specifications of contemporary pavements. Cracks can be seen as a tensile failure in concrete pavement since they are the main source of deterioration and delamination. Any portion of the pavement that experiences tensile loads that are higher than the concrete's flexural strength is vulnerable to cracking. Tensile stresses are produced in rigid pavements due to the weather's impacts and the bending of the concrete base caused by the weight of the vehicles. Previous research demonstrated that the tensile stress generated inside concrete pavements is significantly influenced by the vehicular loads as well as numerous environmental conditions. The severity of fatigue damage is worsened by the simultaneous occurrence of warping stress and wheel load during the day. The stresses present in rigid pavement must be carefully assessed due to

their significant influence on a number of design factors. The effects of traffic load and temperature gradients when combined are not the same sum of those two stresses.

## 2.2 Finite Element Method

Zienkiewicz and Cheung [22] performed one of the earliest studies on the use of FEM for analysing pavements by analysing the behaviour of a pavement under a concentrated load using the thin plate bending theory. Since then, many scientists have utilised FEM to study how pavements react to varied loads. The behaviour of pavements has been studied in great detail through the lens of the first-order shear deformation plate theory.

Chen and Lo [23] employed finite element modelling (FEM) to examine how a pavement will respond to a moving load, based on the first-order shear deformation plate theory. The results showed that the greatest deflection occurred in the middle of the pavement, and the greatest stress was located at the pavement's base. The shear strains in the pavement were also found to be substantial and not to be disregarded.

One other study that employed FEM to examine the thermal behaviour of a pavement when exposed to solar radiation was conducted by Yang et al. By employing a model of the pavement based on the first-order shear deformation plate theory, the study was able to demonstrate that the thermal stress present in the pavement is substantial and may lead to pavement degradation.

Author used FEM to investigate how a moving load and a thermal load interact with a pavement's behaviour. Using a first-order shear deformation plate theory model of the pavement, the study demonstrated that thermal stress significantly altered the pavement's behaviour. The research also demonstrated the need to analyse the pavement with both the dynamic impacts of the moving load and the thermal effects of the sun's radiation taken into account.

A numerical approach for resolving problems that can be stated as functional minimisation or partial differential equations is the finite element method (FEM). A domain of interest is represented by a configuration of finite elements.

There are two aspects of the FEM that deserve special attention:

1) Even with relatively straightforward approximating functions, the piecewise approximation of physical fields on finite elements offers a high level of precision (increasing the number of elements we can achieve any precision).

2) The sparseness of the equation systems for a discretised issue is caused by the locality of the approximation. This makes it easier to tackle problems that include a very high number of unknown nodal values.

Huang [27] developed KENPAVE, a computer programme designed exclusively for pavement analysis. The two primary KENPAVE programmes are KENLAYER and KENSLAB. KENSLAB is used for the analysis of rigid pavements, and KENLAYER is used for the analysis of flexible pavement stresses. The amount of flexural pressure that stiff pavements experience greatly affects how long they can last. Babu et al. examined the effects of flexural stress on rigid pavement by using KENPAVE software to carry out a numerical analysis of pavement and carrying out a comparison analysis with respect to IRC58 rules. They found that the flexural stress for pavement computed with the FEA (Finite Element Analysis) programme KENPAVE is 5 to 6% greater than that calculated with the IRC equation. Ghaffir and Javid used the KENPAVE tool and Westergaard equations to conduct a stress study. Traffic, subgrade soil parameter, PCC (Portland Cement Concrete) slab characteristics, and site-specific climatic data were the variables that the authors compared. The study's conclusions show that the estimated stresses for all key locations produced using Westergaard equations are lower than those obtained using KENPAVE software.

As an alternative to FE analysis, Lee and Darter [28] employed statistical regression technique to create dimensionless parameters and predictive models based on a series of simulations. The concrete slab is treated as a plate that will remain level after bending in all of these 2-D finite element models, which assume that concrete is linear, elastic, and homogenous. However, because the concrete slab is moderately thick, shear deformation has a considerable impact. The nonlinear distribution of temperature fluctuation throughout the depth is challenging to simulate using plate elements, which are unable to represent the stress distribution across its depth. The response of the pavement will be significantly impacted by the surface (smooth or rough) of the concrete slab and base [29].

In a study conducted by Khazanovich et al. [30], the response of concrete pavement to temperature and load strains was investigated using instrumented slabs. Various measuring instruments such as dial gauges, surface-mounted strain gauges, and thermocouples were employed on the test slabs. Dial gauges were utilized to measure curling at the edges and corners of the slabs, while surface-mounted strain gauges were installed along the edges and wheel path to assess the load-induced strains caused by an 80 kN (18 kip) single-axle

load. To monitor pavement temperatures, a thermocouple was placed on the pavement during the tests. Through careful analysis of both observed and analytically generated data, it was determined that the measured deflections exceeded the calculated values, but the measured stresses were lower. A significant finding from the study was that the load configuration had a considerable impact on corner load stresses [31]. According to deductions made by Faraggi et al. (2003), the combined stresses resulting from both load and temperature were lower compared to the individual impacts of each factor occurring simultaneously. Due to the complexity involved, a computer code called RISC was developed using the finite-element method, as it proved challenging to determine the same through analytical methods [32].

IRC uses empirical formula for stress calculation in pavement under different load conditions.

IRC-58[33] suggests following formulas to calculate the maximum tensile stress at the bottom of slab,

Single axle – Pavement with tied concrete shoulders

(a) k ≤ 80 MPa/m

$$S = 0.008 - 6.12\left(\frac{\gamma h^2}{kl^2}\right) + 2.36 \times \frac{Ph}{kl^4} + 0.0266\Delta T$$

(b) k > 80 MPa/m, k ≤ 150 MPa/m

$$S = 0.08 - 9.69\left(\frac{\gamma h^2}{kl^2}\right) + 2.09 \times \frac{Ph}{kl^4} + 0.0409\Delta T$$

(c) k > 150 MPa/m

$$S = 0.042 + 3.26\left(\frac{\gamma h^2}{kl^2}\right) + 1.62 \times \frac{Ph}{kl^4} + 0.0522\Delta T$$

Single axle – Pavement without concrete shoulders

(a) k ≤ 80 MPa/m

$$S = \text{-}0.149 - 2.60\left(\frac{\gamma h^2}{kl^2}\right) + 3.13 \times \frac{Ph}{kl^4} + 0.0297\Delta T$$

(b) k > 80 MPa/m, k ≤ 150 MPa/m

$$S = \text{-}0.119 - 2.99\left(\frac{\gamma h^2}{kl^2}\right) + 2.78 \times \frac{Ph}{kl^4} + 0.0456\Delta T$$

(c) k > 150 MPa/m

$$S = \text{-}0.238 + 7.02\,(\frac{\gamma h^2}{kl^2}) + 2.41 \times \frac{Ph}{kl^4} + 0.0585\Delta T$$

Tandem axle – Pavement with tied concrete shoulders

(a) k ≤ 80 MPa/m

$$S = \text{-}0.188 + 0.93\,(\frac{\gamma h^2}{kl^2}) + 1.025 \times \frac{Ph}{kl^4} + 0.0297\Delta T$$

(b) k > 80 MPa/m, k ≤ 150 MPa/m

$$S = \text{-}0.174 + 1.21\,(\frac{\gamma h^2}{kl^2}) + 0.87 \times \frac{Ph}{kl^4} + 0.0364\Delta T$$

(c) k > 150 MPa/m

$$S = \text{-}0.210 + 3.88\,(\frac{\gamma h^2}{kl^2}) + 0.73 \times \frac{Ph}{kl^4} + 0.0506\Delta T$$

Tandem axle – Pavement without concrete shoulders

(a) k ≤ 80 MPa/m

$$S = \text{-}0.223 + 2.73\,(\frac{\gamma h^2}{kl^2}) + 1.335 \times \frac{Ph}{kl^4} + 0.0229\Delta T$$

(b) k > 80 MPa/m, k ≤ 150 MPa/m

$$S = \text{-}0.276 + 5.78\,(\frac{\gamma h^2}{kl^2}) + 1.14 \times \frac{Ph}{kl^4} + 0.0404\Delta T$$

(c) k > 150 MPa/m

$$S = \text{-}0.3 + 9.88\,(\frac{\gamma h^2}{kl^2}) + 0.965 \times \frac{Ph}{kl^4} + 0.0543\Delta T$$

Also, for the analysis of Top-down cracking IRC-58:2015 provides an expression to calculate the maximum tensile stress at the top of the slab, which is given by,

$$S = \text{-}0.219 + 1.686\left(\frac{\gamma h^2}{kl^2}\right) + 168.48 \times \frac{Ph}{kl^4} + 0.1089\Delta T$$

The symbols in the equations have the following meaning:

S = flexural stress in slab, MPa

ΔT = maximum temperature differential in ºC during day time for bottom-up Cracking.

= sum of the maximum night time negative temperature differential and built in negative temperature differential in ºC for top-down cracking.

h = thickness of slab, m

k = effective modulus of subgrade reaction of foundation, MPa/m

l = radius of relative stiffness = $\{Eh^3/(12k(1-\mu^2)\}0.25$

E = elastic modulus of concrete, MPa

μ = Poisson's ratio of concrete

γ = unit weight of concrete (24 kN/m$^3$, density = 2400 kg/m$^2$)

P = For Bottom-up cracking analysis: - single/tandem rear axle load (kN). No fatigue damage is computed for front (steering) axles for bottom-up cracking case.

= For Top-down cracking analysis: - 100% of rear single axle, 50% of rear tandem axle, 33% of rear tridem axle. Front axle weight is not required to be given as input for top-down cracking case 50% of rear single axle, 25% of rear tandem axle, 16.5% of rear tridem axle, have been considered in the finite element analysis as the front axle weights for single, tandem and tridem rear axles respectively.

B = 0.66 for transverse joint with dowel bars (load transfer efficiency was taken as 50%)

= 0.90 for transverse joint without dowel bars (load transfer efficiency was taken as 10%)

# Chapter 3

# THEORETICAL FORMULATION AND NUMERICAL SCHEME

## 3.1 General

A plate refers to a component that has two large dimensions compared to its thickness, and when subjected to load, it undergoes both bending and stretching. Typically, the thickness of the plate does not exceed one-tenth of its smallest in-plane dimension. Researchers have developed simplified two-dimensional theories to analyse the deformation and stress in plate structures.

The Kirchhoff plate theory or classical plate theory (CPT) is an extension of the Euler Bernoulli beam theory applied to plates.

## 3.2 Classical Plate Theory

Plates are thin, two-dimensional components with one dimension, thickness h, significantly smaller than the other dimensions. They can have straight or curved boundaries and serve as both structural elements and complete structures, such as slab bridges. Plates can have different boundary conditions, including free, supported, and fixed boundaries. The loads on plates are carried by internal bending and torsional moments and transverse shear forces, all perpendicular to the plate surface.

The 'classical plate theory' is a mathematical model used to determine stresses and deformations in thin plates under forces and moments. Love developed this theory in 1888 based on Kirchhoff's assumptions, which represent a three-dimensional plate in two dimensions. The theory assumes that:

1. The material is homogeneous, isotropic, and linear elastic, following Hooke's law.
2. The plate is initially flat.
3. The middle surface of the plate remains unstrained during bending.
4. The thickness of the plate, h, is small compared to its other dimensions.

Specifically, the smallest lateral dimension of the plate is at least ten times larger than its thickness.

Take a plate with a thickness of h that is constant. We will utilise the rectangular Cartesian coordinates (x, y, z), where the z-coordinate is taken positively upward, and the x-y plane coincides with the geometric centre of the plate. Assume that (u, v, w) represents the total displacement of point along the (x, y, z) coordinates. A material point that was at location (x, y, z) in the plate before it was deformed shifts to position (x+u, y+v, z+w). Assuming assumptions 1 and 2, it follows that the thickness normal strain is 0 because a transverse normal is inextensible:

$$\varepsilon_{zz} = \partial w/\partial z = 0$$

which implies that w is independent of z. The third assumption results in zero transverse shear strains

$$\varepsilon_{xz} = \partial u/\partial z + \partial w/\partial x = 0,$$

$$\varepsilon_{yz} = \partial v/\partial z + \partial w/\partial y = 0$$

……..(1)

These conditions, in turn, imply, because w is independent of z, that

$$u(x, y, z) = -z\,\partial w/\partial x + u_0(x, y), \qquad v(x, y, z) = -z\,\partial w/\partial y + v_0(x, y)$$

…….(2)

where $u_0$ and $v_0$ represent the values of u and v, respectively, at the point (x, y, 0). In other words, $u_0$ and $v_0$ denote the displacements along the x and y coordinates, respectively, of a point on the mid-plane.

### 3.2.1 Displacement field and strains

The Kirchhoff hypothesis implies, as discussed above, the following form of the displacement deformations

$$u(x, y, z) = u_0(x, y) - z\left(\frac{\partial W_0}{\partial z}\right)$$

$$v(x, y, z) = v_0(x, y) - z\,\partial w_0/\partial y$$

$$w(x, y, z) = w_0(x, y)$$

(3)

where $(u_0, v_0, w_0)$ represent the displacements in (x, y, z) coordinate directions of a material point at (x, y, 0). Keep in mind that $(u_0, v_0)$ represent the plate's extensional deformation

whereas ($w_0$) represents the deflection caused by bending. Present work uses the small deformation and small strain theory. The linear strain terms can be defined as following:

The strain-displacement relations: -

$$\varepsilon_{xx} = \frac{\partial u}{\partial x} \quad ; \quad \varepsilon_{xy} = \frac{1}{2}\left[\left(\frac{\partial u}{\partial y}\right) + \left(\frac{\partial v}{\partial x}\right) + \left(\frac{\partial w}{\partial x}\frac{\partial w}{\partial y}\right)\right]$$

$$\varepsilon_{yy} = \frac{\partial v}{\partial y} \qquad \varepsilon_{xz} = \frac{1}{2}\left[\left(\frac{\partial u}{\partial z}\right) + \left(\frac{\partial w}{\partial x}\right)\right]$$

$$\varepsilon_{zz} = \frac{\partial w}{\partial z} \qquad \varepsilon_{yz} = \frac{1}{2}\left[\left(\frac{\partial v}{\partial z}\right) + \left(\frac{\partial w}{\partial y}\right)\right]$$

(4&5)

For the displacement field in Eq. (3.3.1), $\partial w/\partial z = 0$. In view of the assumptions, the strains eq. 5 for the displacement field eq.3 reduce to

$$\varepsilon_{xx} = \frac{\partial u_0}{\partial x} - z\frac{\partial^2 w_0}{\partial x^2};$$

$$\varepsilon_{yy} = \frac{\partial v_0}{\partial y} - z\frac{\partial^2 w_0}{\partial y^2};$$

$$\varepsilon_{xy} = \frac{1}{2}\left[\left(\frac{\partial u_0}{\partial y}\right) + \left(\frac{\partial v_0}{\partial x}\right) + \left(\frac{\partial w_0}{\partial x}\frac{\partial w_0}{\partial y} - 2z\frac{\partial^2 w_0}{\partial x\,\partial y}\right)\right];$$

$$\varepsilon_{xz} = \frac{1}{2}\left[-\frac{\partial w_0}{\partial x} + \frac{\partial w_0}{\partial x}\right] = 0;$$

$$\varepsilon_{yz} = \frac{1}{2}\left[-\frac{\partial w_0}{\partial y} + \frac{\partial w_0}{\partial y}\right] = 0;$$

$$\varepsilon_{zz} = 0\ ;$$

(6)

The strains in Eq. 6 have the form

$$\varepsilon_{xx} = \varepsilon^{\circ}_{xx} + z.\varepsilon^{1}_{xx}$$

$$\gamma_{xy} = 2\varepsilon_{xy} = \gamma^{0}_{xy} + z\gamma^{1}_{xy}$$

$$E_{yy} = \varepsilon^{\circ}_{yy} + z.\varepsilon^{1}_{yy}$$

(7)

where the strains of the middle surface, ($\varepsilon^{\circ}_{xx}$ , $\varepsilon^{\circ}_{yy}$ , $\gamma^{0}_{xy}$), are called the membrane strains, and ($\varepsilon^{1}_{xx}$, $\varepsilon^{1}_{yy}$, $\gamma^{1}_{xy}$) are the flexural (bending) strains, known as the curvatures. In matrix notation, Eqs. (7) can be written as

$$\begin{bmatrix}\varepsilon_{xx}\\ \varepsilon_{yy}\\ \gamma_{xy}\end{bmatrix} = \begin{bmatrix}\varepsilon_{xx}^{\circ}\\ \varepsilon_{yy}^{\circ}\\ \gamma_{xy}^{\circ}\end{bmatrix} + z\begin{bmatrix}\varepsilon_{xx}^{1}\\ \varepsilon_{yy}^{1}\\ \gamma_{xy}^{1}\end{bmatrix}$$

(8)

Six variables are reduced to three.

### 3.2.2 Constitutive Stress-Strain Relations: -

Based on the assumptions (3) and (4) the stress–strain relation for plane stress for an FGM plate is

$$\sigma_x = \frac{E(z)}{1-\nu(z)^2}\{\varepsilon_{x_0} + \nu(z)\varepsilon_{x_0} - z[\frac{\partial^2 w}{\partial x^2} + \nu(z)\frac{\partial^2 w}{\partial y^2}]\}$$
$$\sigma_y = \frac{E(z)}{1-\nu(z)^2}\{\varepsilon_{y_0} + \nu(z)\varepsilon_{y_0} - z[\frac{\partial^2 w}{\partial y^2} + \nu(z)\frac{\partial^2 w}{\partial x^2}]\}$$
$$\sigma_x = \frac{E(z)}{1-\nu(z)^2}\left(\frac{1-\nu(z)}{2}\right)[\gamma_{xy} - 2.z.\frac{\partial^2 w}{\partial x \partial y}]$$

(9)

The axial forces, shear forces, and the bending moment of plate

The stress resultants per unit length of the middle surface are defined by integrating stresses along the thickness. The in-plane axial forces Nx, Ny, and Nxy are defined as

$$N_x = \int_{-h/2}^{h/2} \sigma_x dz \qquad N_y = \int_{-h/2}^{h/2} \sigma_y dz \qquad N_{xy} = \int_{-h/2}^{h/2} \tau_{xy} dz$$

The transverse shear force $V_x$ and $V_y$ are defined as

$$V_x = \int_{-h/2}^{h/2} \tau_{xz} dz \qquad V_y = \int_{-h/2}^{h/2} \tau_{yz} dz$$

And the bending moments $M_x$, $M_y$ and $M_{xy}$ ared defined as

$$N_x = \int_{-h/2}^{h/2} z\sigma_x dz \qquad N_y = \int_{-h/2}^{h/2} z\sigma_y dz \qquad N_{xy} = \int_{-h/2}^{h/2} z\tau_{xy} dz$$

(10)

The sign conventions of the axial and shear forces are illustrated in Fig. 2.1 and that of the bending moment are shown in Fig. 2.2.

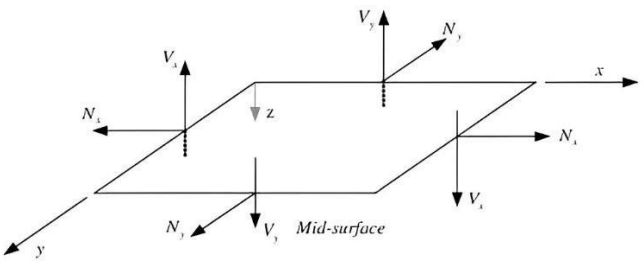

Fig 2.1 The positive directions of the axial and shear forces in plates( JN Reddy).

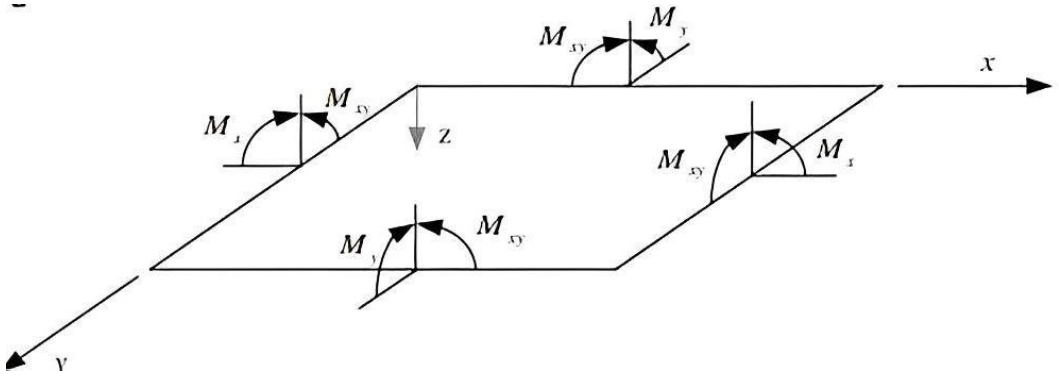


Fig. 2.2 moments in plates [9]

By substituting of Eq. (9) to Eqs. (10), we obtain the axial forces matrix and the bending moments in the matrix forms as follows:

$$\begin{Bmatrix} N_x \\ N_y \\ N_{xy} \end{Bmatrix} = \begin{bmatrix} A_{11} & A_{12} & 0 \\ A_{12} & A_{11} & 0 \\ 0 & 0 & A_{66} \end{bmatrix} \begin{Bmatrix} \varepsilon_{x_o} \\ \varepsilon_{y_o} \\ \gamma_{xy_o} \end{Bmatrix} + \begin{bmatrix} B_{11} & B_{12} & 0 \\ B_{12} & B_{11} & 0 \\ 0 & 0 & B_{66} \end{bmatrix} \begin{Bmatrix} -\frac{\partial^2 w}{\partial x^2} \\ -\frac{\partial^2 w}{\partial y^2} \\ -2\frac{\partial^2 w}{\partial x \partial y} \end{Bmatrix} \quad (11)$$

$$\begin{Bmatrix} M_x \\ M_y \\ M_{xy} \end{Bmatrix} = \begin{bmatrix} B_{11} & B_{12} & 0 \\ B_{12} & B_{11} & 0 \\ 0 & 0 & B_{66} \end{bmatrix} \begin{Bmatrix} \varepsilon_{x_o} \\ \varepsilon_{y_o} \\ \gamma_{xy_o} \end{Bmatrix} + \begin{bmatrix} C_{11} & C_{12} & 0 \\ C_{12} & C_{11} & 0 \\ 0 & 0 & C_{66} \end{bmatrix} \begin{Bmatrix} -\frac{\partial^2 w}{\partial x^2} \\ -\frac{\partial^2 w}{\partial y^2} \\ -2\frac{\partial^2 w}{\partial x \partial y} \end{Bmatrix} \quad (12)$$

where the coefficients of $A_{ij}$, $B_{ij}$ and $C_{ij}$ are the integration of the material properties of the plate and they are

$$A_{11} = \int_{-h/2}^{h/2} \frac{E(z)}{1-\nu(z)^2} dz \; ; \; A_{12} = \int_{-h/2}^{h/2} \frac{E(z).\nu(z)}{1-\nu(z)^2} dz \; ; \; B_{11} = \int_{-h/2}^{h/2} \frac{z.E(z)}{1-\nu(z)^2} dz$$

$$B_{12} = \int_{-h/2}^{h/2} \frac{z.E(z).\nu(z)}{1-\nu(z)^2} dz; \quad C_{11} = \int_{-h/2}^{h/2} \frac{z^2.E(z)}{1-\nu(z)^2} dz \ ;$$

$$C_{12} = \int_{-h/2}^{h/2} \frac{z^2.E(z).\nu(z)}{1-\nu(z)^2} dz \ ; A_{66} = \int_{-h/2}^{h/2} \frac{z^2.E(z)}{1-\nu(z)^2} \left(\frac{1-\nu(z)}{2}\right) dz;$$

$$B_{66} = \int_{-h/2}^{h/2} \frac{z.E(z)}{1-\nu(z)^2} \left(\frac{1-\nu(z)}{2}\right) dz \; C_{66} = \int_{-h/2}^{h/2} \frac{z^2.E(z)}{1-\nu(z)^2} \left(\frac{1-\nu(z)}{2}\right) dz$$

(13)

### 3.2.3 The equilibrium and compatibility equations of plate: -

Assume that the distributed loads qx, qy, and qz are applied to the FGM plate in the x, y, and z directions. Think of a little solid element having dx, dy, and dz dimensions. Figure depicts every force operating on the little element. The resultant forces in the x-direction must be zero when the element is in equilibrium, i.e.

$$\left(N_x + \frac{\partial N_x}{\partial x} dx\right) dy + \left(N_{yx} + \frac{\partial N_{yx}}{\partial y} dx\right) dx - N_x dy - N_{yx} dx + q_x dx dy = 0$$

(14)

Or

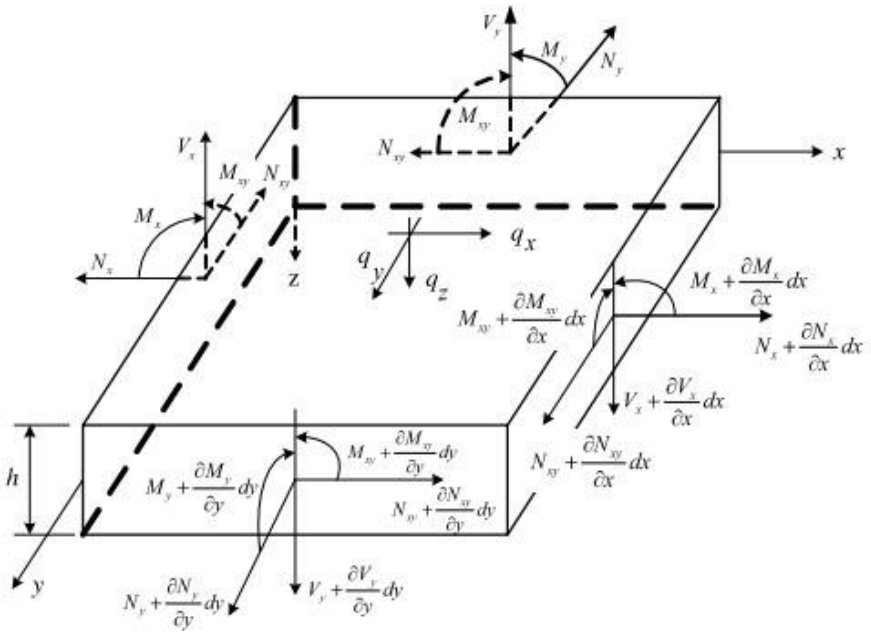


Fig.3.1 The forces in a small element dx-dy-dz of plate [9].

$$\frac{\partial N_x}{\partial x}+\frac{\partial N_{yx}}{\partial y}+q_x\ =0$$

Similarly, the zero forces in y- and z-directions yield:

$$\frac{\partial N_{yx}}{\partial x}+\frac{\partial N_y}{\partial y}+q_y\ =0 \qquad\qquad \frac{\partial V_x}{\partial x}+\frac{\partial V_y}{\partial y}+q_z\ =0$$

(15)

Additionally, two equilibrium equations are produced by the zero resultant moments in the y- and x-directions.

$$V_x=\frac{\partial M_x}{\partial x}+\frac{\partial M_{xy}}{\partial y} \qquad ; \qquad V_y=\frac{\partial M_{xy}}{\partial x}+\frac{\partial M_y}{\partial y}$$

(16)

Resultant of above three equations

$$\frac{\partial^2 M_x}{\partial x^2}+2\frac{\partial^2 M_{xy}}{\partial x\partial y}+\frac{\partial^2 M_y}{\partial y^2}=-q_z(x,y)$$

(17)

Eq. (17) contains three moment components; therefore, deformation must be taken into account. Equations (12) and (17) can be changed to

$$B_{11}\left(\frac{\partial^2 \varepsilon_x{}^o}{\partial x^2}+\frac{\partial^2 \varepsilon_y{}^o}{\partial y^2}\right)+B_{12}\left(\frac{\partial^2 \varepsilon_x{}^o}{\partial y^2}+\frac{\partial^2 \varepsilon_y{}^o}{\partial x^2}\right)+2B_{66}\frac{\partial^2 \gamma_{xy}{}^o}{\partial x\partial y}-C_{11}\frac{\partial^4 w}{\partial x^4}$$
$$-(2C_{11}+4C_{66})\frac{\partial^4 w}{\partial x^2\partial y^2}-C_{11}\frac{\partial^4 w}{\partial y^4}=-q_z(x,y)$$

(18)

The in plane equations (15) can be solved in terms of a stress function ø(x,y) if the FGM plate is solely under the transverse load qz, or qx = 0 and qy = 0.

$$N_x\ =\frac{\partial^2 \phi}{\partial y^2}\ ;\ N_x\ =\frac{\partial^2 \phi}{\partial y^2};\ N_{xy}\ =\frac{\partial^2 \phi}{\partial x\partial y}$$

(19)

The strains at the middle surface are then represented in terms of the stress function ø(x,y) and the deflection w using Eqs. (10) and (19).

$$\begin{Bmatrix} \varepsilon_{x_0} \\ \varepsilon_{y_0} \\ \gamma_{xy_0} \end{Bmatrix} = \begin{bmatrix} P_{11} & P_{12} & 0 \\ P_{12} & P_{11} & 0 \\ 0 & 0 & P_{66} \end{bmatrix} \begin{Bmatrix} \frac{\partial^2 \phi}{\partial y^2} \\ \frac{\partial^2 \phi}{\partial x^2} \\ \frac{\partial^2 \phi}{\partial x \partial y} \end{Bmatrix} + \begin{bmatrix} Q_{11} & Q_{12} & 0 \\ Q_{12} & Q_{11} & 0 \\ 0 & 0 & Q_{66} \end{bmatrix} \begin{Bmatrix} -\frac{\partial^2 w}{\partial x^2} \\ -\frac{\partial^2 w}{\partial y^2} \\ -2\frac{\partial^2 w}{\partial x \partial y} \end{Bmatrix}$$

(20)

The bending moments are rearranged by substituting Eq. (20) into (12) as

$$\begin{Bmatrix} M_x \\ M_y \\ M_{xy} \end{Bmatrix} = \begin{bmatrix} -Q_{11} & -Q_{12} & 0 \\ -Q_{12} & -Q_{11} & 0 \\ 0 & 0 & -Q_{66} \end{bmatrix} \begin{Bmatrix} \frac{\partial^2 \phi}{\partial x^2} \\ \frac{\partial^2 \phi}{\partial y^2} \\ 2\frac{\partial^2 \phi}{\partial x \partial y} \end{Bmatrix} + \begin{bmatrix} S_{11} & S_{12} & 0 \\ S_{12} & S_{11} & 0 \\ 0 & 0 & S_{66} \end{bmatrix} \begin{Bmatrix} -\frac{\partial^2 w}{\partial x^2} \\ -\frac{\partial^2 w}{\partial y^2} \\ -2\frac{\partial^2 w}{\partial x \partial y} \end{Bmatrix} \quad (21)$$

Where,

$P_{11} = A_{11}/\Delta$

$P_{12} = -A_{12}/\Delta$

$P_{66} = -1/A_{66}$

$Q_{11} = (A_{12}B_{12} - A_{11}B_{11}) / \Delta$

$Q_{12} = (A_{12}B_{11} - A_{11}B_{12}) / \Delta$

$Q_{66} = -B_{66} / A_{66}$

$S11 = B_{11}Q_{11} + B_{12}Q_{12} + C_{11}$

$S_{12} = B_{11}Q_{12} + B_{12}Q_{11} + C_{12}$

$S66 = C_{66} + B_{66}Q_{66}$

$\Delta = (A_{11})^2 - (A_{12})^2$

Equation (23) is substituted into equation (21) to obtain the relationship between stress function ø(x,y) and deflection w:

$$Q_{12}\frac{\partial^4 \phi}{\partial x^4} + 2(Q_{11} - Q_{66})\frac{\partial^4 \phi}{\partial x^2 \partial y^2} + Q_{12}\frac{\partial^4 \phi}{\partial y^4} + S_{11}\frac{\partial^4 w}{\partial x^4} + 2(S_{12} + 2S_{66})\frac{\partial^4 w}{\partial x^2 \partial y^2} + S_{11}\frac{\partial^4 w}{\partial y^4} = q_z(x, y)$$

(22)

Since the stress function ø(x,y) and the deflection w in Eq. (25) are unknown, one more equation is needed. A compatibility equation is then used to provide the governing equation for ø(x,y). By using Eq. (7), the compatibility equation

$$\frac{\partial^2 s_x}{\partial y^2} + \frac{\partial^2 s_y}{\partial x^2} = \frac{\partial^2 \gamma_{xy}}{\partial x \partial y} \tag{23}$$

can be expressed as

$$\frac{\partial^2 s_x}{\partial y^2}^{o} + \frac{\partial^2 s_y}{\partial x^2}^{o} = \frac{\partial^2 \gamma_{xy}}{\partial x \partial y}^{o} \tag{24}$$

Consequently, substituting Eq. (23) into Eq. (26) gives the relation between stress function ø(x,y) and the deflection w:

$$P_{11}\frac{\partial^4 \phi}{\partial x^4} + (2p_{12} - P_{66})\frac{\partial^4 \phi}{\partial x^2 \partial y^2} + P_{11}\frac{\partial^4 \phi}{\partial y^4} - Q_{12}\frac{\partial^4 w}{\partial x^4} - 2(Q_{11} - Q_{66})\frac{\partial^4 w}{\partial x^2 \partial y^2} - Q_{12}\frac{\partial^4 w}{\partial y^4} = 0 \tag{25}$$

Eqs. (25) and (27) provide the simultaneous equations to solve the stress function ø(x,y) and the deflection w.

### 3.3 The First Order Shear Deformation Theory

It is an assumption of the classical plate theory (CPT) that plane sections will initially be normal to the mid surface of a plate before deviating after deformation, the plane of that surface and the normal to that surface's orientation both stay unchanged. This is the consequence of not taking into account transverse shear strains. Nevertheless, non-negligible shear deformations occur in plates that are thick or moderately thick, and the theory produces false findings for laminated plate configurations. Therefore, it should come as no surprise that transverse shear deformations are required to be accounted for in the study. The Reissner and Mindlin model [1–3] are one of the more well-known plate theories. This model is a first order shear deformation theory (FSDT) [4,5] and it interprets the displacement field as linear variations of midplane displacements. According to this theory, the shear correction factors have an effect on the link that exists between the resultant shear forces and the shear strains.

### 3.3.1 The equilibrium and compatibility equations of plate: -

According to the traditional plate theory and taking into account the impact of transverse shear deformations, the displacement field of a rectangular plate can be written as

$$u(x,y,z) = u_o(x,y) + z\left[\alpha \frac{\partial w_o}{\partial x} + \beta\theta_x\right]$$
$$v(x,y,z) = v_o(x,y) + z\left[\alpha \frac{\partial w_o}{\partial y} + \beta\theta_x\right]$$
$$w(x,y,z) = w_o(x,y) \tag{26}$$

where the corresponding midplane displacements in the x, y, and z directions are denoted by the letters $u_0$(x, y), $v_0$(x, y), and $w_0$(x, y), and the letters x and y signify the rotations of midplane normal about the y and x axes. The generic displacement field shown above includes both the CPT and FSDT theories, as follows:

Classical plate theory (CPT): $\alpha = -1$, $\beta = 0$

First order shear deformation theory (FSDT): $\alpha = 0$, $\beta = 1$.

### 3.3.2 The strains-stress relation of displacement fields

$$\varepsilon_x = \frac{\partial u}{\partial x} - z\frac{\partial^2 w_b}{\partial x^2}$$
$$\varepsilon_y = \frac{\partial v}{\partial y} - z\frac{\partial^2 w_b}{\partial y^2}$$
$$\gamma_{xy} = \frac{\partial u}{\partial x} + \frac{\partial v}{\partial y} - 2z\frac{\partial^2 w_b}{\partial x \partial y}$$
$$\gamma_{xz} = \frac{\partial w_s}{\partial x}$$
$$\gamma_{xz} = \frac{\partial w_s}{\partial y} \tag{27}$$

Stress: -

$$\begin{matrix}\sigma_x \\ \sigma_y \\ \tau_{xy} \\ \tau_{xz} \\ \{\tau_{xz}\}\end{matrix} = \frac{E(z)}{1-\nu^2}\begin{bmatrix} 1 & \nu & 0 & 0 & 0 \\ \nu & 1 & 0 & 0 & 0 \\ 0 & 0 & \frac{1-\nu}{2} & 0 & 0 \\ 0 & 0 & 0 & \frac{1-\nu}{2} & 0 \\ 0 & 0 & 0 & 0 & \frac{1-\nu}{2} \end{bmatrix}\begin{matrix}\varepsilon_x \\ \varepsilon_y \\ \gamma_{xy} \\ \gamma_{xz} \\ \{\gamma_{yz}\}\end{matrix} \tag{28}$$

The principle of virtual displacements for a laminated plate resting on elastic foundation can be stated in analytical form as:

$$\int_{-h/2}^{h/2} \int_{A} (\sigma_x \delta\varepsilon_x + \sigma_y \delta\varepsilon_y + \tau_{xy}\delta\gamma_{xy} + \tau_{xz}\delta\gamma_{xz} + \tau_{yz}\delta\gamma_{yz}) dA dz + \frac{1}{2}\int (k_o w_o + k_1 A^2 w_o) dA + \int q_o \delta w dA = 0 \quad (29)$$

in which $w_0$ is vertical displacement of mid plane of the plate, $k_0$ is Winkler modulus, $k_1$ is the shear modulus of foundation and

$$\nabla^2 = \frac{\partial^2}{\partial x^2} + \frac{\partial^2}{\partial y^2} \quad (30)$$

If equation (2) is written in terms of stress and moment resultants and integrated by parts then collecting the coefficients of δu, δv, δw, δθx and δθy, equilibrium equations are obtained as;

$$\frac{\partial N_x}{\partial x} + \frac{\partial N_{xy}}{\partial y} = 0$$

$$\frac{\partial N_{xy}}{\partial x} + \frac{\partial N_y}{\partial y} = 0$$

$$\frac{\partial Q_x}{\partial x} + \frac{\partial Q_y}{\partial y} + q_o + k_o w_o - k_1 A^2 w_o = 0$$

$$\frac{\partial M_x}{\partial x} + \frac{\partial M_{xy}}{\partial y} - Q_x = 0$$

$$\frac{\partial M_{xy}}{\partial y} + \frac{\partial M_y}{\partial y} - Q_y = 0 \quad (31)$$

### 3.3.3 Temperature effect

All displacement term will remain same and strain value changes with addition of (-αΔT). So, after consideration of temperature new stress strain relations

$$\begin{Bmatrix} \sigma_x \\ \sigma_y \\ \tau_{xy} \end{Bmatrix} = \begin{bmatrix} Q_{11} & Q_{12} & 0 \\ Q_{12} & Q_{22} & 0 \\ 0 & 0 & Q_{66} \end{bmatrix} \begin{Bmatrix} \varepsilon_x - \alpha T \\ \varepsilon_y - \alpha T \\ \gamma_{xy} \end{Bmatrix} \text{ and } \begin{Bmatrix} \tau_{yz} \\ \tau_{xz} \end{Bmatrix} = \begin{bmatrix} Q_{44} & 0 \\ 0 & Q_{55} \end{bmatrix} \begin{Bmatrix} \gamma_{yz} \\ \gamma_{xz} \end{Bmatrix}$$

Using Hamilton's principle governing equations of the plate can be derived as

$$\int_0^T \left(\delta U + \delta V - \delta K\right) dt = 0$$

$$\frac{1}{2}\iiint [\sigma_x(\varepsilon_x - \alpha\Delta T) + \sigma_x(\varepsilon_x - \alpha\Delta T) + \tau_{xy}\gamma_{xy} + \tau_{xy}\gamma_{xy} + \tau_{xy}\gamma_{xy}]$$

$$+\frac{1}{2}\int (k_o w_o + k_1 \nabla^2 w_o)\, dA + \int q_o \delta w dA = 0$$

(32)

This equation is a form of the principle of virtual work, which is a fundamental principle in mechanics used to calculate the equilibrium conditions of a system. It is used in the analysis of structures subjected to external loads.

The equation represents the balance of internal and external work done on a three-dimensional plate. The left-hand side of the equation represents the internal work done by the stresses and strains in the material, while the right-hand side represents the external work done by external loads and boundary conditions.

The first term,

$$[\sigma_x(\varepsilon_x - \alpha\Delta T) + \sigma_x(\varepsilon_x - \alpha\Delta T) + \tau_{xy}\gamma_{xy} + \tau_{xy}\gamma_{xy} + \tau_{xy}\gamma_{xy}]$$

represents the internal work done by stresses and strains in the material. It includes contributions from normal and shear stresses and strains, as well as the effect of temperature changes (represented by the term $\alpha\Delta T$, where $\alpha$ is the coefficient of thermal expansion and \mathrm{\Delta T} is the temperature change).

### 3.3.4 Elastic foundation effect

$$(k_o w_o + k_1 \nabla^2 w_o) dA$$

Represents he external work done by body forces acting on the solid. It represents the volume integral of the product of the elastic foundation coefficient and the displacement vector (w).

$k_o$ is the Winkler coefficient, which represents the stiffness of the elastic foundation. It is a constant that characterizes the relationship between the deflection of the plate and the reaction force exerted by the foundation on the plate. $w_o$ is the deflection of the plate at its center, caused by a uniformly distributed load over the entire surface of the plate. $k_1$ is the

Pasternak coefficient, which accounts for the non-uniform distribution of the load on the plate. It characterizes the relationship between the deflection of the plate and the reaction force exerted by the foundation on the plate when the load is not uniformly distributed. $A^2\ w_o$ is the Laplacian of the deflection of the plate, which describes the curvature of the deflection profile. It is a second-order partial derivative of the deflection function with respect to the x and y coordinates of the plate. $dA$ is the infinitesimal area element of the plate.

### 3.3.5 External applied load

The third term, $\int q_o \delta w dA$ represents the external work done by point loads acting on the solid. The symbol $q_o \delta w$ represents the point load, and $\delta w$ is the displacement vector due to the point load. The dot product with dA represents the surface area element over which the point load is applied.

In summary, equation (32) represents the total potential energy of an elastic solid subject to thermal and mechanical loading. It consists of three terms representing the internal energy, the potential energy stored in the elastic foundation, and the potential energy stored in the applied loads. The equation can be used to determine the equilibrium configuration of the solid under given loading conditions.

# Chapter 4

# WORK METHODOLOGY

## 4.1 Generation of Dataset and processing

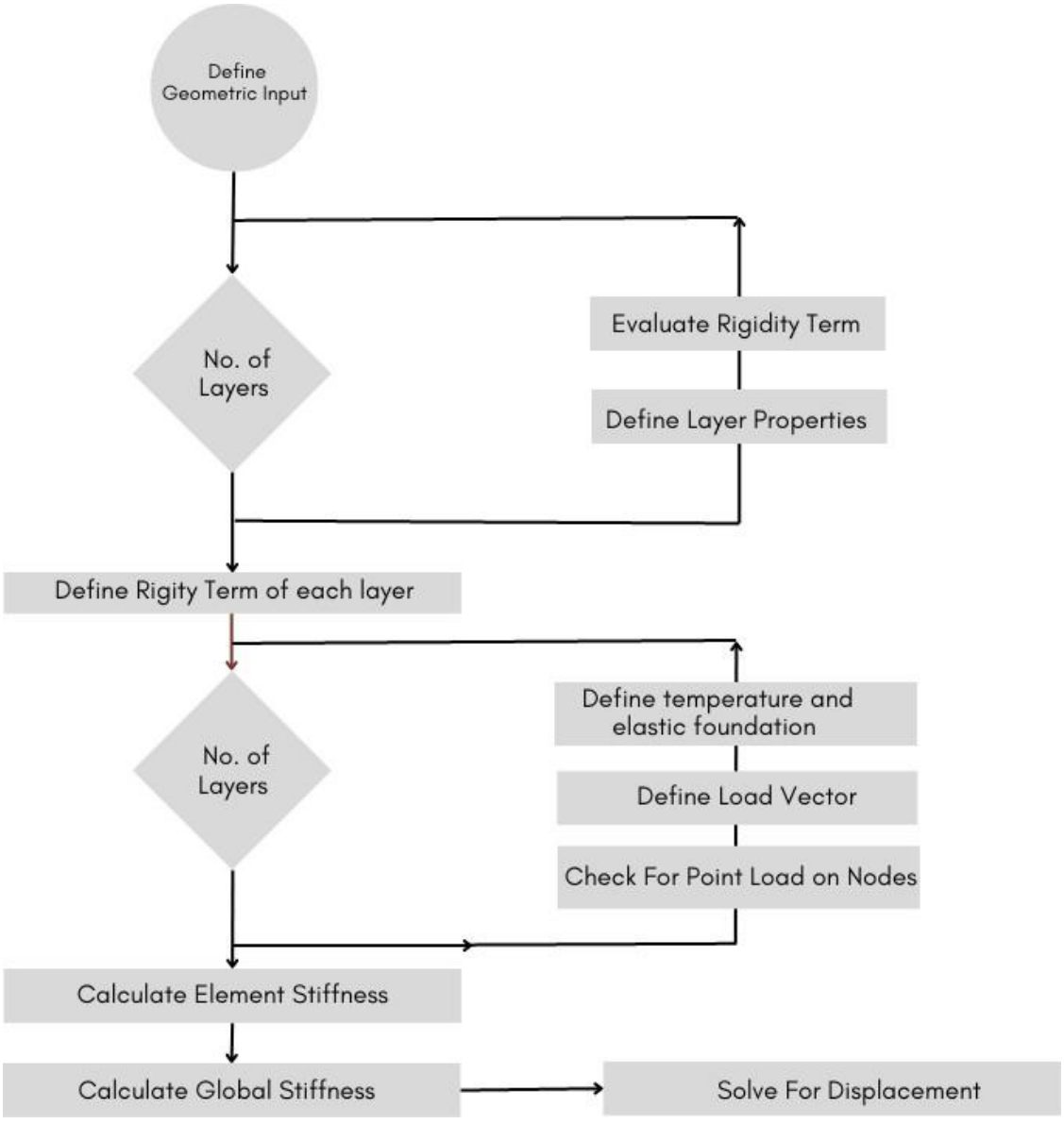


Figure 3 Work-Methodology

The process for plate analysis using a Finite Element Method (FEM) code can be outlined as follows:

1. Input the geometric details of the plate: Specify the dimensions, shape, and boundary conditions of the plate, such as length, width, and any constraints or supports.
2. Define layer properties: Specify the material properties for each layer of the plate, such as Young's modulus and Poisson's ratio. The plate may consist of multiple layers with different material properties.
3. Calculate layer stiffness: Utilize the layer properties to determine the stiffness matrix for each layer. The stiffness matrix describes the relationship between applied forces and resulting deformations in each layer.
4. Input loading conditions: Define the applied loads on the plate, such as point loads, distributed loads, or pressure loads. Specify the magnitude, direction, and location of each load.
5. Input temperature conditions: Consider the effects of temperature on the plate. Specify the temperature distribution across the plate and its variations over time. Thermal expansion coefficients may also be required to account for thermal effects on material properties.
6. Consider elastic foundation effects: If the plate is resting on an elastic foundation, input the foundation details, such as stiffness or spring constants. This accounts for the interaction between the plate and the underlying support.
7. Calculate element stiffness matrix: Based on the plate geometry, layer stiffness, loading conditions, temperature effects, and elastic foundation details, compute the element stiffness matrix for each finite element. The element stiffness matrix represents the relationship between nodal displacements and nodal forces within each element.
8. Assemble the global stiffness matrix: Combine the element stiffness matrices to form the global stiffness matrix of the entire plate. This matrix represents the overall stiffness and interactions between all elements in the system.
9. Solve for displacements: Apply appropriate boundary conditions and solve the system of equations formed by the global stiffness matrix. This yields the displacements at each node of the plate.

By following these steps, the FEM code can analyse the plate and provide valuable information about its behaviour under different loading, temperature, and foundation conditions.

From displacement results stresses and post processing is done.

1. Gather pavement parameters: The initial step is to collect the required pavement parameters from the user. Variations in temperature, material qualities, and pavement layer thickness all play a role.
2. Finite element model development: A finite element model of the pavement will be created using a programme that accommodates the first order shear deformation plate theory, once the parameters of the pavement have been collected. Boundary conditions, element type, size, and mesh density from the preceding results will all form the basis of the model.
3. Stiffness matrix formation: The pavement structure's stiffness matrix will be constructed by combining the existing stiffness matrices of the model's constituent elements. Adjustments to the stiffness matrix will be made to accommodate a variety of loads, including elastic, thermal, and point loads. By summing the matrices for elastic loading, thermal loading, and uniform distribution load, we obtain the global stiffness matrix.
4. Solution of the finite element model: In order to determine the nodal displacements and associated stresses and strains in the pavement structure, the finite element model will be solved using numerical techniques after the stiffness matrix has been formed. The nodal displacements are used in conjunction with the deformation matrix to determine the strains.
5. Results Analysis: The behaviour of the pavement under various loading circumstances will be evaluated by analysing the results of the finite element study. This involves assessing the overall performance of the pavement structure and locating any locations of significant stress or deformation.

## 4.2 Derivation of the element stiffness matrix

we are analysing an eight-nodded element using FEM. Eight-nodded elements are commonly used in FEM simulations as they provide a good balance between computational efficiency and accuracy. The element is defined by eight nodes, with each node having five degrees of freedom (DOF) - translation in the u, v, w, $\theta_x$ and $\theta_y$ . The stiffness matrix describes the element's behaviour, which relates the nodal displacements to the nodal forces. By analysing the stiffness matrix using FEM, we can accurately predict the deformation and stress behaviour of the eight-nodded element under different loading

conditions. This information is crucial in designing and optimising engineering structures for optimal performance and safety.

### 4.3 Numerical scheme

The current study employs a continuous displacement model known as the first-order shear deformation theory (FSDT). To formulate the finite element method, shape functions are utilized, resulting in a robust FEM code. An eight-noded element with isoperimetric formulation (as depicted in the figure) is used to solve the governing equations. The plate domain is divided into a finite number of elements, and within each element, the degree of freedom can be expressed as:

$$\mathrm{U}(x,y) = \sum_{i=1}^{n} N_i U_i$$

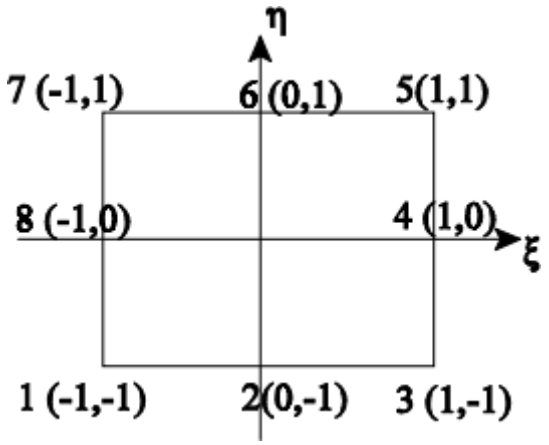


Where U is the dependent variable, Ni interpolation function(shape function) associated with the i th node of the element, "n" is number of nodes in one element.

After simplification:

$$\mathrm{U} = N_1U_1 + N_2U_2 + N_3U_3 + N_4U_4 + N_5U_5 + N_6U_6 + N_7U_7 + \mathrm{N}_8U_8$$

Similarly for V, W, $\theta_x$ and $\theta_y$.

$$\begin{bmatrix} U \\ V \\ W \\ \theta_x \\ [\theta_y] \end{bmatrix} = \begin{matrix} N_{1-8} & 0 & 0 & 0 & 0 \\ 0 & N_{1-8} & 0 & 0 & 0 \\ 0 & 0 & N_{1-8} & 0 & 0 \\ 0 & 0 & 0 & N_{1-8} & 0 \\ \{0 & 0 & 0 & 0 & N_{1-8}\} \end{matrix} \begin{bmatrix} U_{1-8} \\ V_{1-8} \\ W_{1-8} \\ \theta_{x1-8} \\ [\theta_{y1-8}] \end{bmatrix}$$

Strain relation can be written as:

$$\varepsilon_{xx} = \frac{dU}{dx}\,;\varepsilon_{yy} = \frac{dV}{dx}\,;\varepsilon_{xy} = \frac{dU}{dy} + \frac{dV}{dx}$$

From previous discussion we can write

$$\begin{bmatrix}\varepsilon_{xx}\\ \varepsilon_{yy}\\ \varepsilon_{xy}\end{bmatrix} = \begin{bmatrix}1 & 0 & 0 & z & 0 & 0\\ 0 & 1 & 0 & 0 & z & 0\\ 0 & 0 & 1 & 0 & 0 & z\end{bmatrix} \begin{bmatrix}(\varepsilon^o)_x\\ (\varepsilon^o)_y\\ (\varepsilon^o)_{xy}\\ \kappa_x\\ \kappa_y\\ \kappa_{xy}\end{bmatrix}$$

After putting the value of U in above equation

Let's $dnx = \frac{dN_i}{dx}\,;\; dny = \frac{dN_i}{dy}$

$$\begin{bmatrix}(\varepsilon^o)_x\\ (\varepsilon^o)_y\\ (\varepsilon^o)_{xy}\\ \kappa_x\\ \kappa_y\\ \kappa_{xy}\end{bmatrix} = \begin{bmatrix}dnx_{1-8} & 0_{1-8} & 0_{1-8} & 0_{1-8} & 0_{1-8}\\ 0_{1-8} & dny_{1-8} & 0_{1-8} & 0_{1-8} & 0_{1-8}\\ dny_{1-8} & dnx_{1-8} & 0_{1-8} & 0_{1-8} & 0_{1-8}\\ 0_{1-8} & 0_{1-8} & 0_{1-8} & dnx_{1-8} & 0_{1-8}\\ 0_{1-8} & 0_{1-8} & 0_{1-8} & 0_{1-8} & dny_{1-8}\\ 0_{1-8} & 0_{1-8} & 0_{1-8} & dny_{1-8} & dnx_{1-8}\end{bmatrix} \begin{bmatrix}U_{1-8}\\ V_{1-8}\\ W_{1-8}\\ \theta_{x1-8}\\ \theta_{y1-8}\end{bmatrix}$$

Above matrix expression can be written as $\varepsilon_{s(6\times1)} = Bbarb_{(6\times40)} * D_{(40\times1)}$ for shear term.

$$\begin{bmatrix}\varepsilon_{xx}\\ \varepsilon_{yy}\\ \varepsilon_{xy}\end{bmatrix} = \begin{bmatrix}(\varepsilon^o)_x\\ (\varepsilon^o)_y\\ (\varepsilon^o)_{xy}\end{bmatrix} + z.\begin{bmatrix}K_x\\ K_y\\ K_{xy}\end{bmatrix} = B_1.D + z.B_2.D$$

$$\begin{bmatrix}\varepsilon_{xz}\\ \varepsilon_{yz}\end{bmatrix} = \begin{bmatrix}0_{1-8} & 0_{1-8} & dnx_{1-8} & N_{1-8} & 0_{1-8}\\ 0_{1-8} & 0_{1-8} & dny_{1-8} & 0_{1-8} & N_{1-8}\end{bmatrix} \begin{bmatrix}U_{1-8}\\ V_{1-8}\\ W_{1-8}\\ \theta_{x1-8}\\ \theta_{y1-8}\end{bmatrix}$$

Similarly, for $\varepsilon_{b(2\times1)} = BbarS_{(2\times40)} * D_{(40\times1)}$ for bending term

Combining both strain relationships

$$\begin{pmatrix} \varepsilon_b \\ \varepsilon_s \end{pmatrix} = \begin{bmatrix} Bbarb \\ Bbars \end{bmatrix} * D$$

Stress strain constitutive relation:

$$\begin{bmatrix} \sigma_{xx} \\ \sigma_{yy} \\ \sigma_{xy} \end{bmatrix} = \begin{bmatrix} Q_{11r} & Q_{12r} & Q_{14r} \\ Q_{12r} & Q_{22r} & Q_{24r} \\ Q_{14r} & Q_{24r} & Q_{44r} \end{bmatrix} \begin{bmatrix} \varepsilon_{xx} \\ \varepsilon_{yy} \\ \varepsilon_{xy} \end{bmatrix} = Q_b * \varepsilon_b$$

$$= Q_b * Bbarb * D$$

$$\begin{bmatrix} \tau_{xz} \\ \tau_{yz} \end{bmatrix} = \begin{bmatrix} Q_{55r} & Q_{56r} \\ Q_{56r} & Q_{66r} \end{bmatrix} \begin{bmatrix} \varepsilon_{xz} \\ \varepsilon_{yz} \end{bmatrix} = Q_s * \varepsilon_s = Q_s * Bbars * D$$

### 4.4 Deriving stiffness matrix from governing equation

$$\delta\Pi = \delta U + \delta V = 0$$

$$\delta U = \int \delta\varepsilon^T * \sigma * dv = \int \delta\varepsilon^T * \sigma_b * dv + \int \delta\varepsilon^T * \sigma_s * dv$$

$$\delta U = \int \delta(Bbarb * D)^T * \sigma_b * dv + \int \delta(Bbars * D)^T * \sigma_s * dv$$

$$\delta U = \int (Bbarb * \delta D)^T * \sigma_b * dv + \int (Bbars * \delta D)^T * \sigma_s * dv$$

$$\delta U = \int \delta D^T * Bbarb^T * \sigma_b * dv + \int \delta D^T * Bbars^T * \sigma_s * dv$$

$$\delta U = \int \delta D^T * Bbarb^T * Q_b * \text{Bbarb} * \text{D} * dv + \int \delta D^T * Bbars^T * Q_s$$

$$* \text{Bbars} * \text{D} * d$$

$$\delta U = \delta D^T \int (B_1{}^T + Z * B_2{}^T) * Q_b * (B_1{}^T + Z * B_2{}^T) * \text{D} * dv$$

$$+ \delta D^T \int Bbars^T * Q_s * \text{Bbars} * \text{D} * dv$$

$$\delta U = \delta D^T \left[\int \left[\int (B_1{}^T + Z * B_2{}^T) * Q_b * (B_1{}^T + Z * B_2{}^T) * dz\right] da\right] D$$

$$+ \delta D^T \left[\int \left[\int Bbars^T * Q_s * \text{Bbars} * dz\right] da\right] D$$

$$\delta U = \delta D^T \left[\iint (B_1{}^T * Q_b * B_1 + B_1{}^T * Q_b * Z * B_2 + Z * B_2{}^T * Q_b * B_1 \right.$$

$$\left. + Z^2 * B_2{}^T * Q_b * B_2) dz * da\right] D$$

$$+ \delta D^T \left[\int \left[\int Bbars^T * Q_s * \text{Bbars} * dz\right] da\right] D$$

$$putting\ A = Q_b * h\ and\ F = Q_b * \frac{h^3}{12}$$

$$= \delta D^T \left[\int (B_1{}^T * \text{A} * B_1 + 0 + 0 + B_2{}^T * F * B_2) dz * da\right] D$$

$$+ \delta D^T \left[\int \left[\int Bbars^T * Q_s * \text{Bbars} * dz\right] da\right] D$$

After simplification

$$\boldsymbol{\delta U = \delta D^T \left[\int (\mathbf{B}^T * \mathbf{E} * \mathbf{B}) da\right] D}$$

$$\delta V = -\int \delta U^T * P * da = -\int (N * \delta D)^T * P * da$$

$$\boldsymbol{\delta V = -\delta D^T \int N^T * P * da}$$

Where P is the node load vector.

$$\delta \Pi = \delta U + \delta V = 0$$

$$\boldsymbol{\delta \Pi = \delta D^T \left[\int (\mathbf{B}^T * \mathbf{E} * \mathbf{B}) da\right] D - \delta D^T \int N^T * P * da}$$

Now,

$\text{K}_\text{e} = \int (\text{B}^T * \text{E} * \text{B}) da$ where $\text{K}_\text{e}$ is the stiffness matrix.

Converting the above expression from the global coordinate system to local natural coordinate system by gauss integration method.

$$K_e = \int_{-1}^{1}\int w_{a*} w_{b*} B^T * D * B * |J| * \partial\xi * \partial\eta$$

Where $w_a\ and\ w_b$ are weighted functions and $|J|$ is a determinant of the Jacobian matrix.

**4.1 Derivation of the stiffness matrix of elastic foundation:**

$$P_f = K_w * w - K_p * (\frac{\partial^2 w}{\partial x^2} + \frac{\partial^2 w}{\partial y^2})$$

*where,* $K_w = winkler\ foundation\ coefficient$

$K_p = Pasternak\ foundation\ cofficient$

By minimum energy principle:

$$U = \frac{1}{2}\int P_f * w * dx.dy = \frac{1}{2}\int P_f * w * dA$$

$$\delta U = \int P_f * w * dA$$

$$\delta U = \int K_w * w * \delta w * dA - \int K_p * \frac{\partial^2 w}{\partial x^2} * \delta w * dA - \int K_p * \frac{\partial^2 w}{\partial y^2} * \delta w * dA$$

*converting it into weak form*

$$\delta U = \int K_w * w * \delta w * dA - \int K_p [\frac{\partial}{\partial x}(\frac{\partial w}{\partial x} * \delta w) - \frac{\partial w}{\partial x} * \frac{\partial \delta w}{\partial x}] - \int K_p [\frac{\partial}{\partial y}(\frac{\partial w}{\partial y} * \delta w) - \frac{\partial w}{\partial y} * \frac{\partial \delta w}{\partial y}]$$

$$\delta U = \int K_w * w * \delta w * dA - \int K_p (\frac{\partial w}{\partial x} * \delta w)\, dy + \int K_p (\frac{\partial w}{\partial x} * \frac{\partial \delta w}{\partial x})\, dA - \int K_p (\frac{\partial w}{\partial y} * \delta w)\, dx + \int K_p (\frac{\partial w}{\partial x} * \frac{\partial \delta w}{\partial x})\, dA$$

$$\delta U = K_w * N^T * N + K_p (\frac{\partial N^T}{\partial x} * \frac{\partial N}{\partial x} + \frac{\partial N^T}{\partial y} * \frac{\partial N}{\partial y})$$

$$\delta U = K_w * N^T * N + K_p * dnx^T * dnx + K_p * dny^T * dny$$

$$K_{elastic\ foundation} = K_w * N^T * N + K_p * dnx^T * dnx + K_p * dny^T * dny$$

### 4.5 Derivation of stiffness matrix for thermal load:

The stiffness matrix for thermal load can be derived by considering the virtual work done by thermal loads on the system.

The thermal load vector $P_t$ is similarly computed as

$$P_t = \iint_{-1}^{1} w_{a*} w_{b*} B^T * N_{thermal} * |J| * \partial\xi * \partial\eta$$

$$N_{thermal} = \int [N_{xT} \quad N_{yT} \quad N_{xyT} \quad M_{xT} \quad M_{yT} \quad M_{xyT}]^T dz$$

as discussed earlier these are stress and moment resultants.

$$\begin{bmatrix} N_{xT} \\ N_{yT} \\ N_{xyT} \\ M_{xT} \\ M_{yT} \\ [M_{xyT}] \end{bmatrix} = \begin{bmatrix} 1 & 0 & 0 & z & 0 & 0 \\ 0 & 1 & 0 & 0 & z & 0 \\ 0 & 0 & 1 & 0 & 0 & z^2 \end{bmatrix}^T \begin{bmatrix} Q_{11r} & Q_{12r} & Q_{41r} \\ Q_{12r} & Q_{22r} & Q_{24r} \\ Q_{14r} & Q_{24r} & Q_{44r} \end{bmatrix} \begin{bmatrix} a_1 \\ a_2 \\ a_{12} \end{bmatrix} * F(t)$$

Where F(t) is temperature variation function along z direction.

# Chapter 5
# NUMERICAL RESULTS

A computer programme has been created that provides an analytical solution for the bending of laminated plates supported by an elastic basis. A numerical example (Example1) was solved in order to confirm the program's accuracy, and the effect of foundation stiffness and fibre orientations on plate bending was examined. The outcomes were compared to those attained using the Finite Element Method after that.

Figure 1. In this illustration, a square plate that is symmetrically laminated (0/90/0)s, simply supported, and resting on a Winkler foundation (k0=100 Pa/m, k1=0) is taken into account. The material parameters of each layer are as follows: E1=181106 kN/m2, E2=10.3106 kN/m2, G12=7.17106 kN/m2, and v12=0.28. All the layers are the same thickness. The plate has a side length of 12 m. The force applied to the plate is uniformly distributed, q=1 kN/m2. The problem is resolved using the finite element approach and the current method (using the ANSYS computer programmes) for verification, and the outcomes are compared. The 12 x 12 finite element mesh is utilised in the finite element analysis.

The displacement distributions along the x-axis of the plate are given in Figures 3–6 for two different foundation stiffnesses.

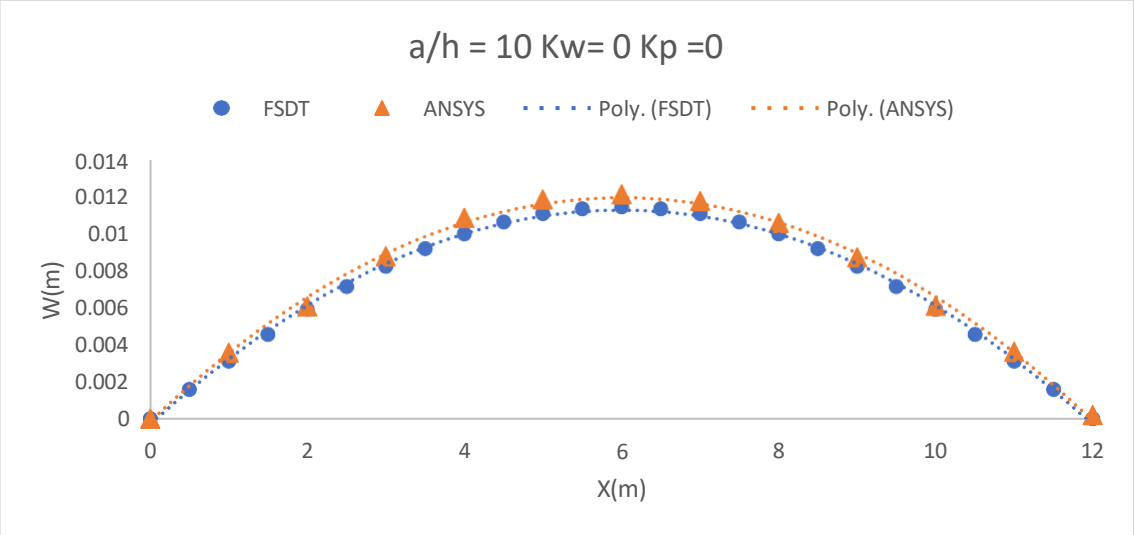


Figure 4 The displacement without elastic foundation (a/h = 10) at y=6m.

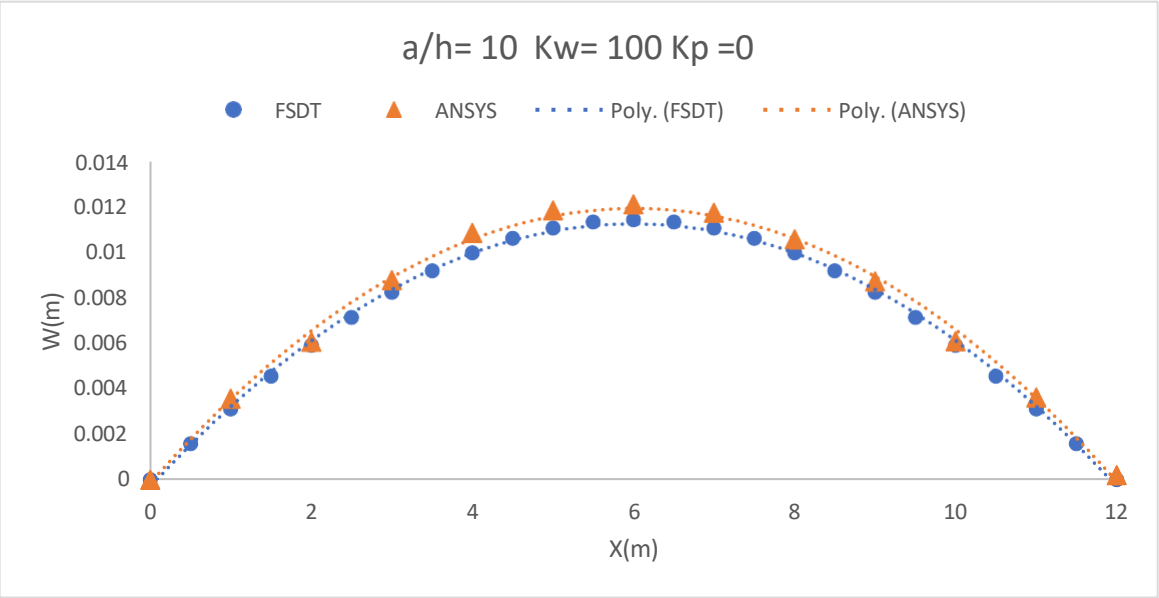


Figure 5 The displacement without elastic foundation (a/h = 10) at y=6m.

According to the graph, it can be observed that the effect of elastic foundation is not evident when the length to thickness ratio is less. The graph shows that as the length to thickness ratio decreases, the difference in the deflection of the plate with and without the elastic foundation becomes negligible. This means that when the length to thickness ratio is less, the influence of the elastic foundation is not significant enough to affect the deflection of the plate.

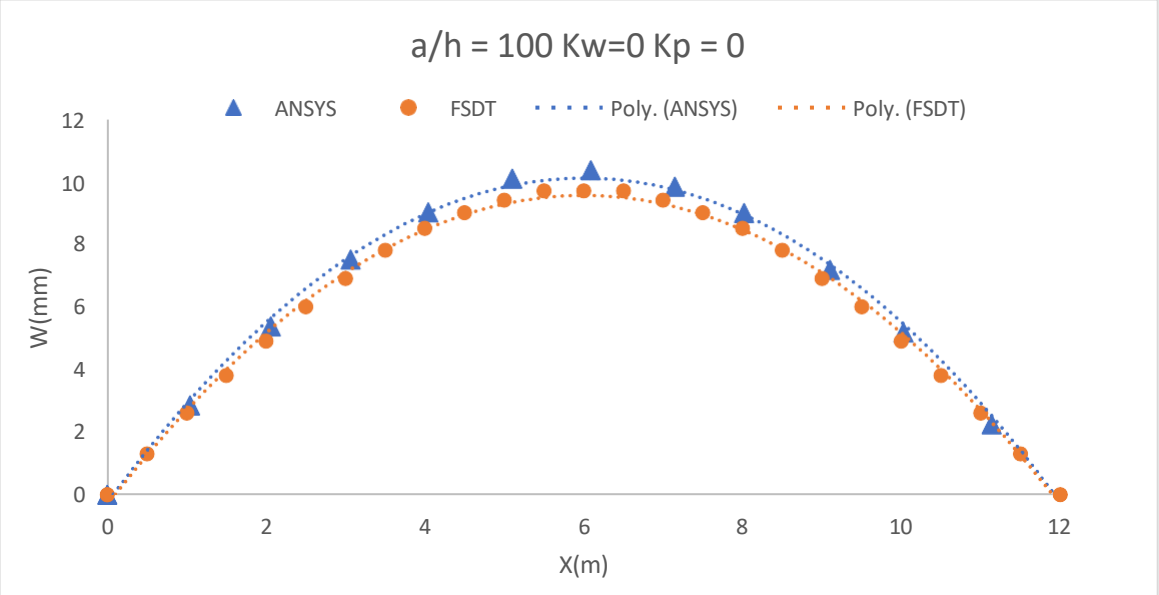


Figure 6 The displacement without elastic foundation (a/h = 100) at y=6m.

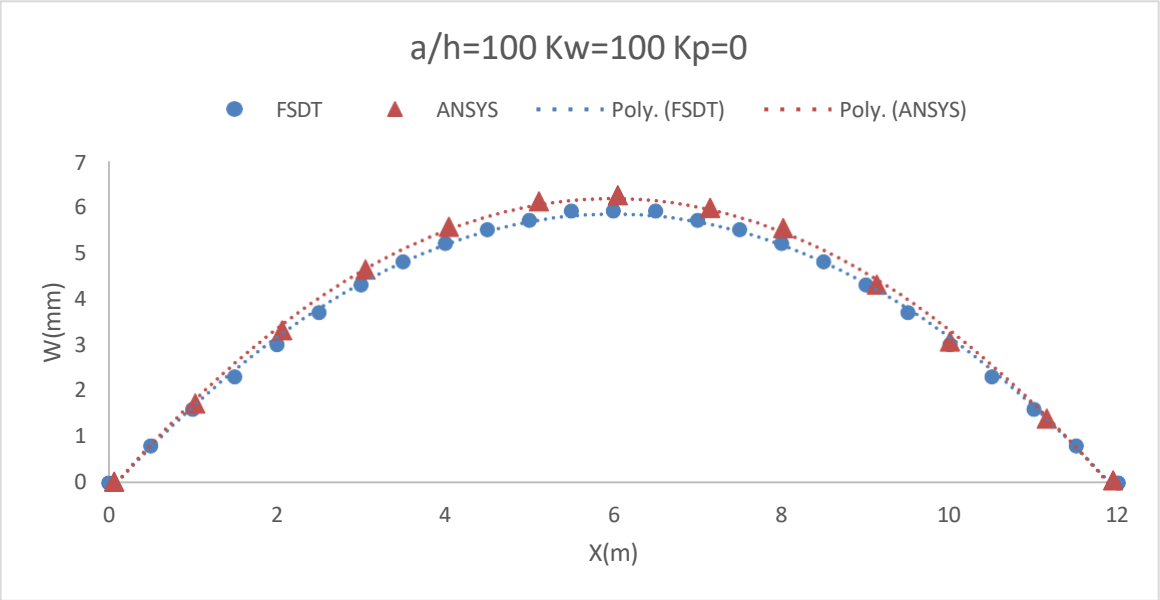


Figure 7 The displacement without elastic foundation (a/h = 100) at y=6m.

The deflection of an elastically supported plate gets more noticeable as its length to height ratio increases, as shown in the same graph. The deflection of the plate on an elastic foundation is much less than the deflection of the plate without a base as the ratio grows. Since the plate is bending less, it follows that the elastic base is doing its job. So, an elastic base can help lessen the plate's deflection and strengthen the plate's stability when the plate's length-to-height ratio is large.

The stress distributions along the x-axis of the plate are given in Figures 8– 15 for two different foundation stiffnesses.

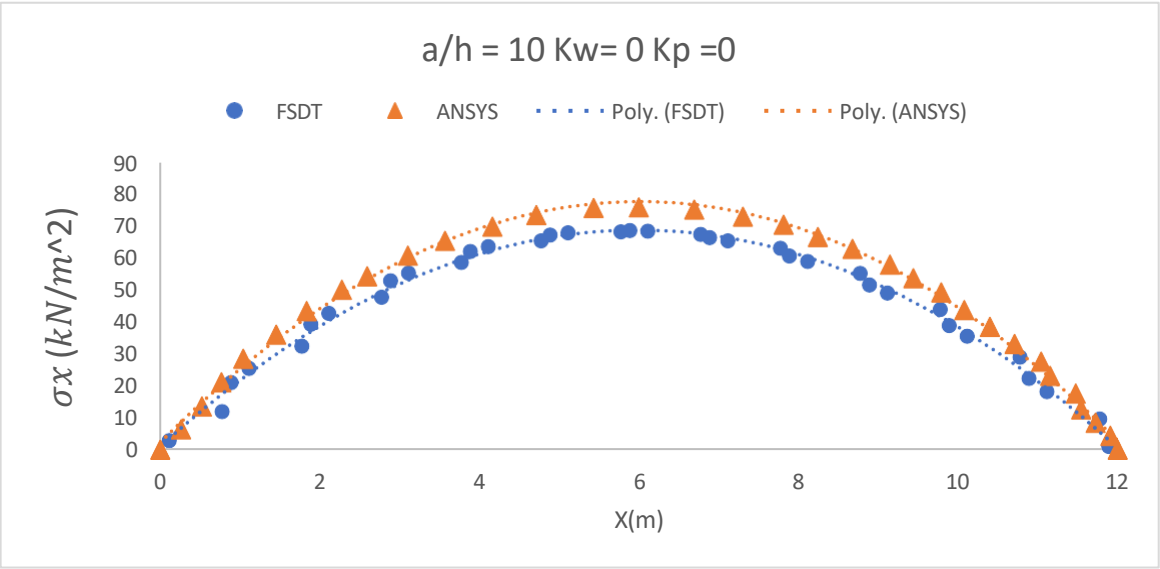


Figure 8 Stress ($\sigma_x$) without elastic foundation (a/h = 10) at h/2 at y=6m.

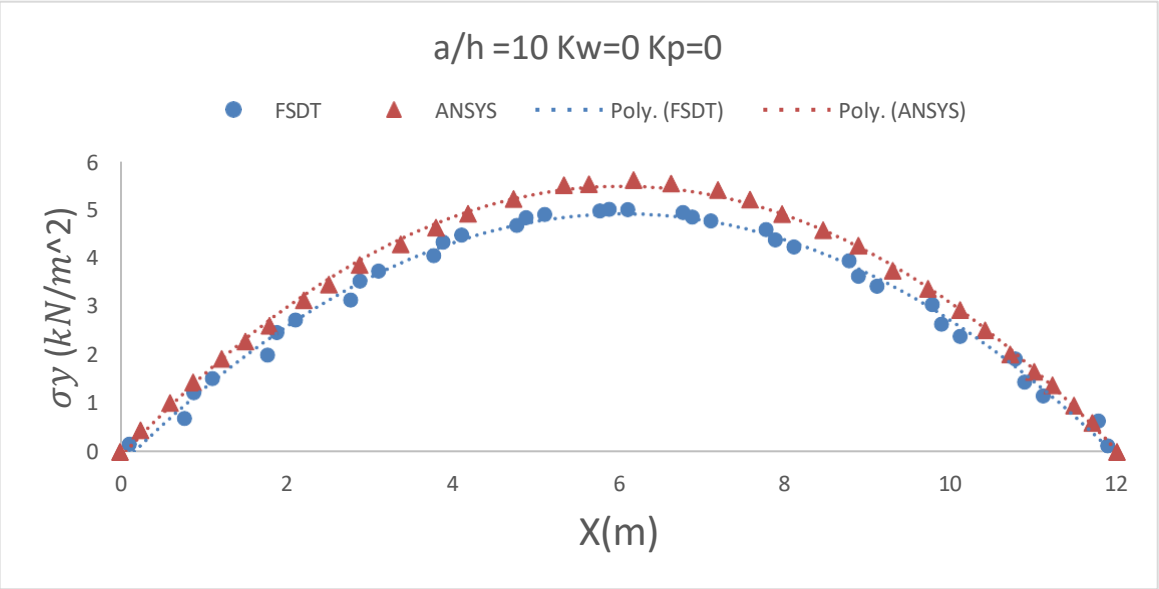


Figure 9 Stress ($\sigma_y$) without elastic foundation (a/h = 10) at h/2 at y=6m.

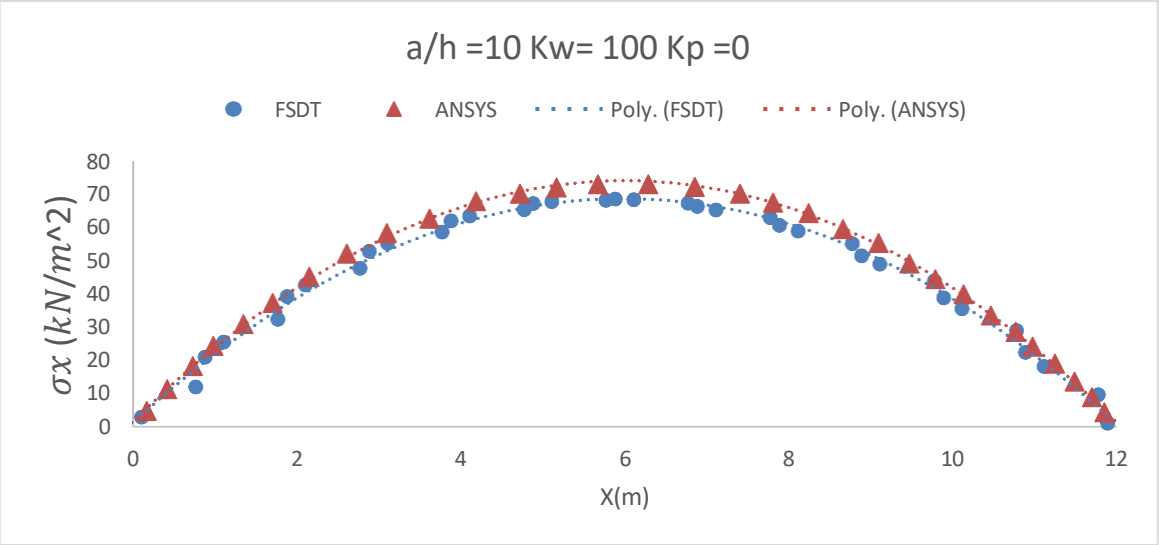


Figure 10 Stress ($\sigma_x$) with elastic foundation (a/h = 10) at h/2 at y=6m.

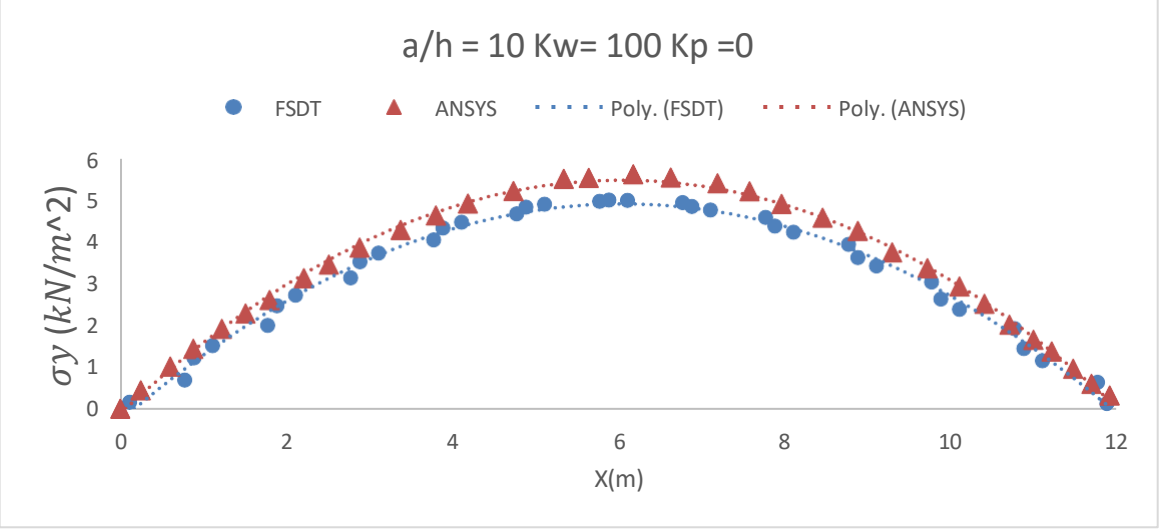


Figure 11 Stress ($\sigma_y$) with elastic foundation (a/h = 10) at h/2 at y=6m.

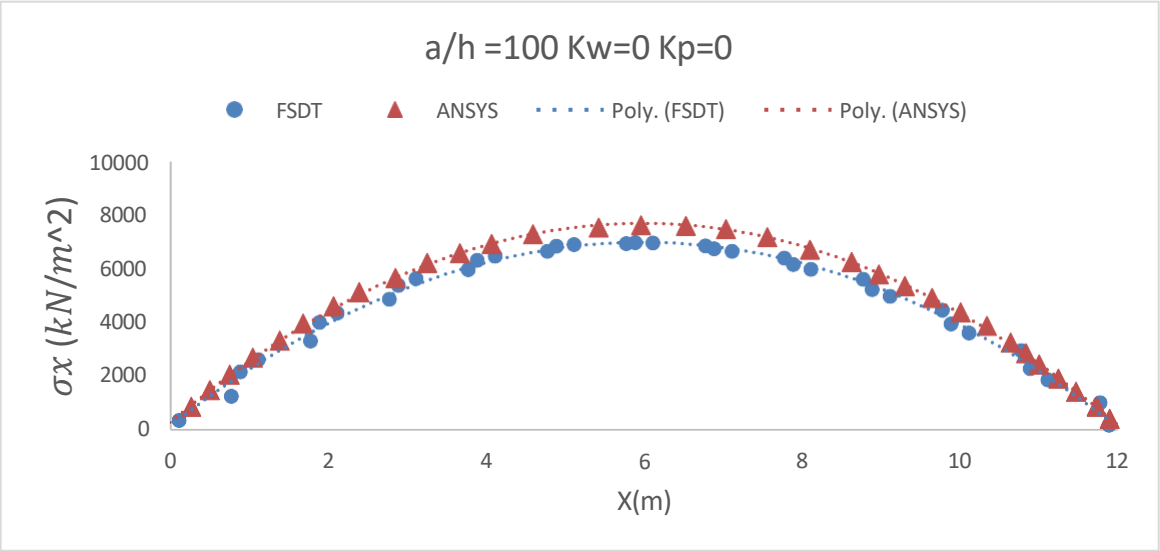


Figure 12 Stress ($\sigma_x$) without elastic foundation (a/h = 100) at h/2 at y=6m.

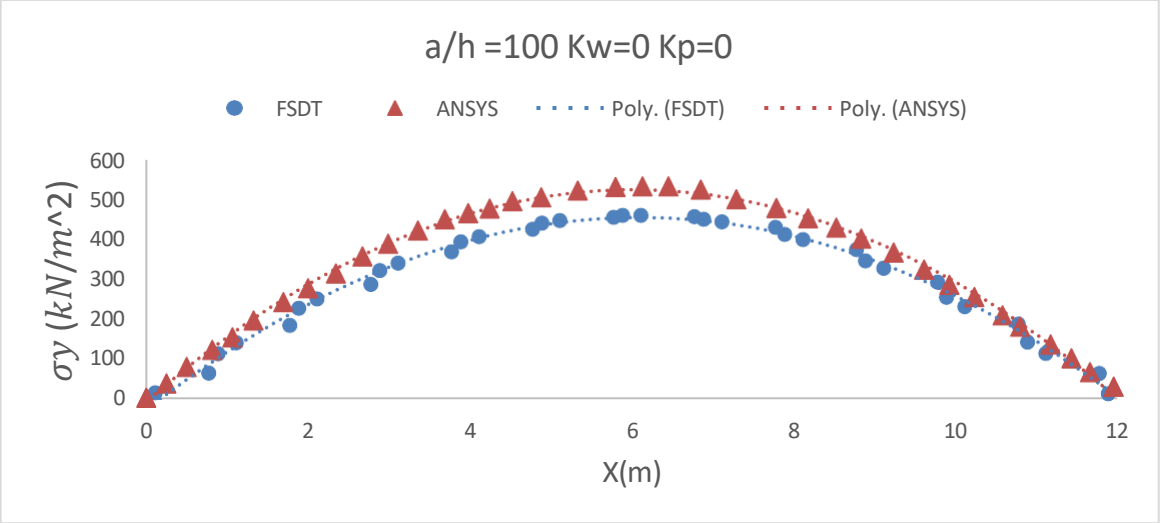


Figure 13 Stress ($\sigma_y$) without elastic foundation (a/h = 100) at h/2 at y=6m.

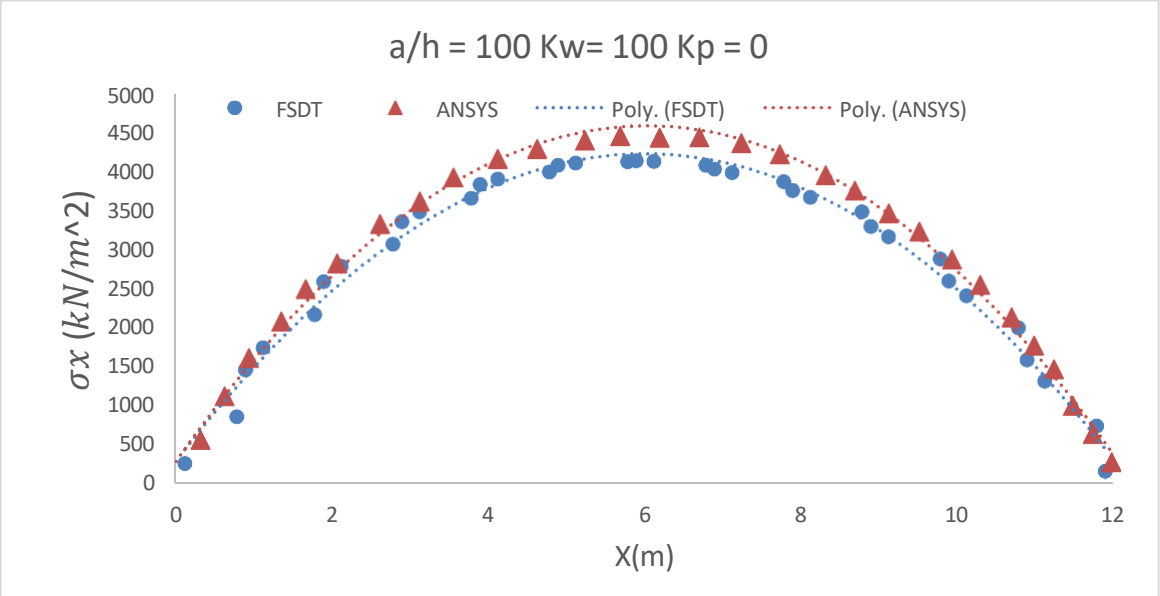


Figure 14 Stress ($\sigma_x$) with elastic foundation (a/h = 100) at h/2 at y=6m.

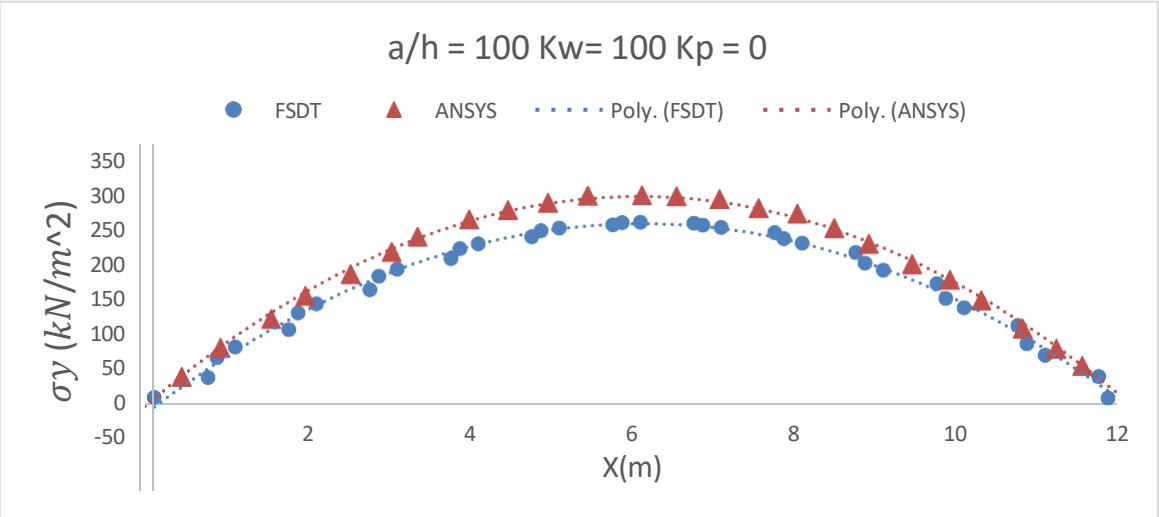


Figure 15 Stress ($\sigma_y$) with elastic foundation (a/h = 100) at h/2 at y=6m.

The stresses of an elastically supported plate get more noticeable as its length to height ratio increases, as shown in the graph. The deflection of the plate on an elastic foundation is much less than the deflection of the plate without a base as the ratio grows. Since the plate is bending less, it follows that the elastic base is doing its job. So, an elastic base can help lessen the plate's stress and strengthen the plate's stability when the plate's length-to-height ratio is large.

Example 2. This example considers a laminated and simply supported (4.5 x 3.5) m plate. The thickness of the layers is 200mm, 150mm, 150mm, and 750mm from top to bottom. The scale is subjected to a point load of 40 kN at centre of plate.

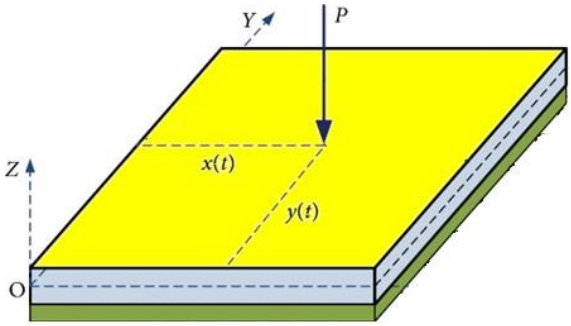


Figure 16 Point load on plate.

The deflection distributions along the x-axis of the plate are given in Figures 16–18 for two different foundation stiffnesses.

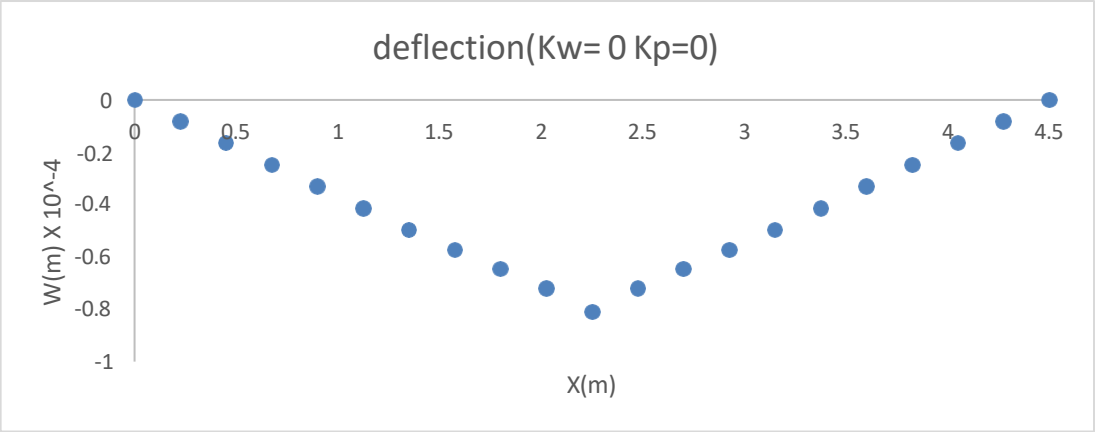


Figure 17 Deflection under point load without elastic foundation from code

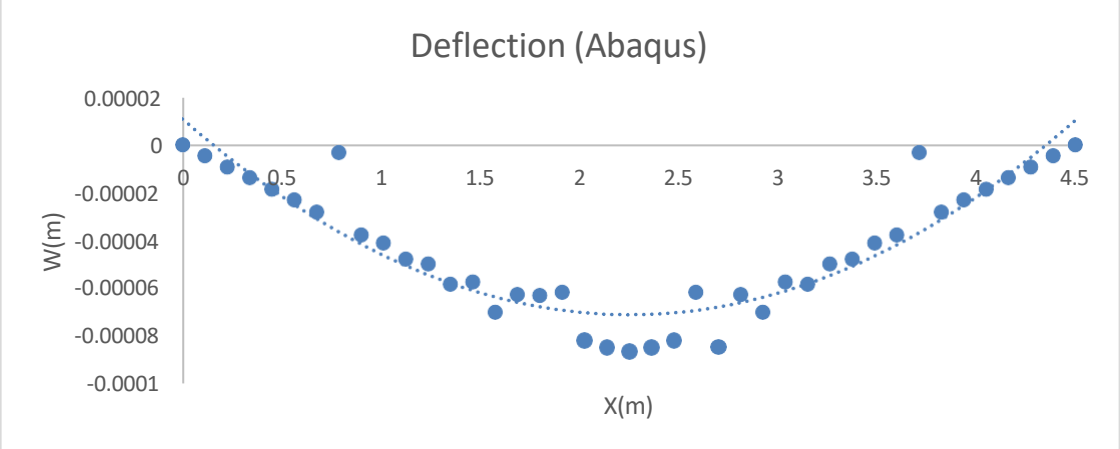


Figure 18 Deflection under point load without elastic foundation from abaqus.

This result valids the point load application of the FSDT code.

Deflection when two 40KN is applied on both side of centre:

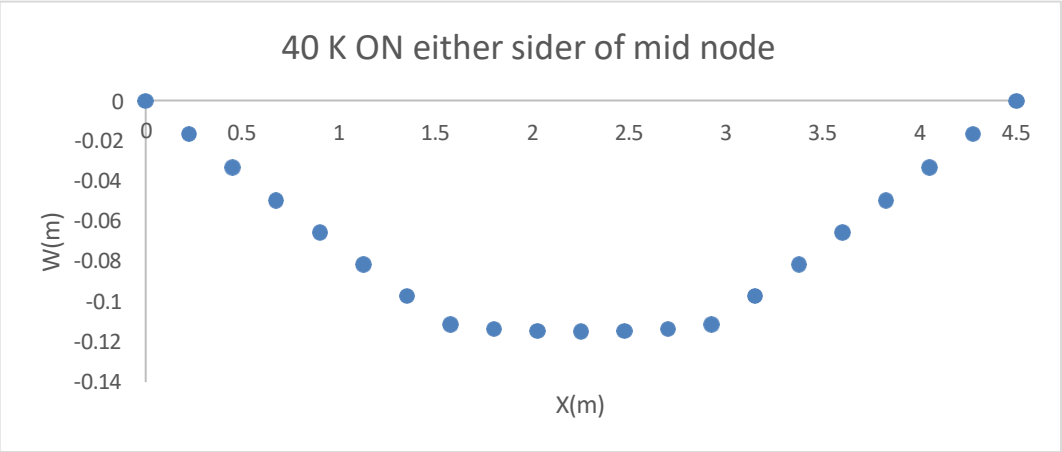


Figure 19 Deflection under two point loads without elastic foundation

Example 3. This example considers a laminated and simply supported plate (pavement) resting on a Winkler foundation (k0=100 Pa/m, k1=100). The thickness of the layers are 200mm, 150mm, 150mm, and 750mm from top to bottom; their material properties are shown in the figure below. The dimension of the plate is (4.5 x 3.5 )m. The scale is subjected to a point load of 40 kN. In the finite element analysis, the 10×10 finite element mesh is used.

Table 1 Pavement Composition and material properties

| Layer | Modulus (Pa) | Poison's Ratio | Density (kN\m^3) | Thickness(mm) |
|---|---|---|---|---|
| PQC | $30*10^9$ | 0.15 | 2300 | 200 |
| DLC | $7*10^9$ | 0.15 | 2100 | 150 |
| Granular Subbase | $2*10^9$ | 0.35 | 2000 | 150 |
| Subgrade | $5*10^7$ | 0.35 | 1800 | 750 |

In this study, the layers which were provided in the model are the Subgrade, Granular subbase (GSB), Dry Lean Concrete (DLC), and PQC (Pavement Quality concrete).

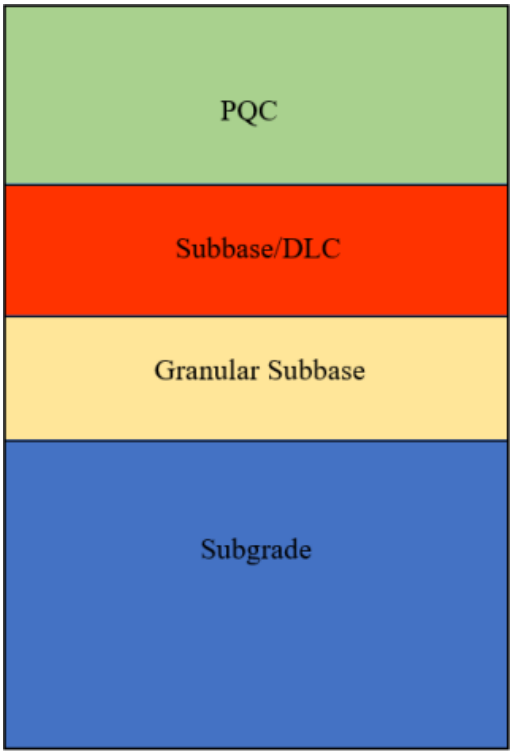


Figure 20 Pavement composition and material properties

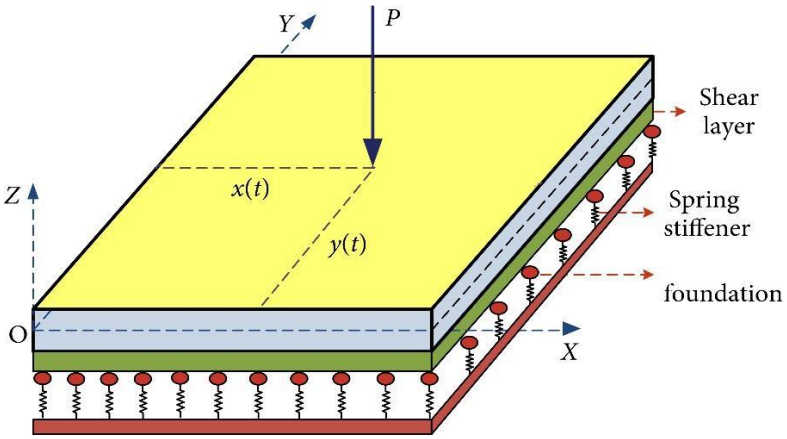


Figure 21 Plate resting on the elastic foundation subjected load.

The displacement distributions along the x-axis of the plate are given in Figures 16–6 for two different foundation stiffnesses.

Now normalising our (a/h) = 1 and getting the deflection profile on diffferent a/h ratio.

Table 2 Comparision of deflection with diffferent elastic foundation condition.

| a/h | Kw=0 | Kw=100 |
|---|---|---|
| 1 | 8E-06 | 8E-06 |
| 2 | 0.0006 | 0.0006 |
| 10 | 0.0674 | 0.0674 |
| 20 | 0.5381 | 0.5359 |
| 30 | 1.8133 | 1.7886 |
| 40 | 4.2922 | 4.1564 |
| 50 | 8.3722 | 7.8715 |
| 60 | 14.449 | 13.024 |
| 70 | 22.916 | 19.543 |
| 80 | 34.166 | 27.218 |
| 90 | 48.589 | 35.745 |
| 100 | 66.575 | 44.803 |

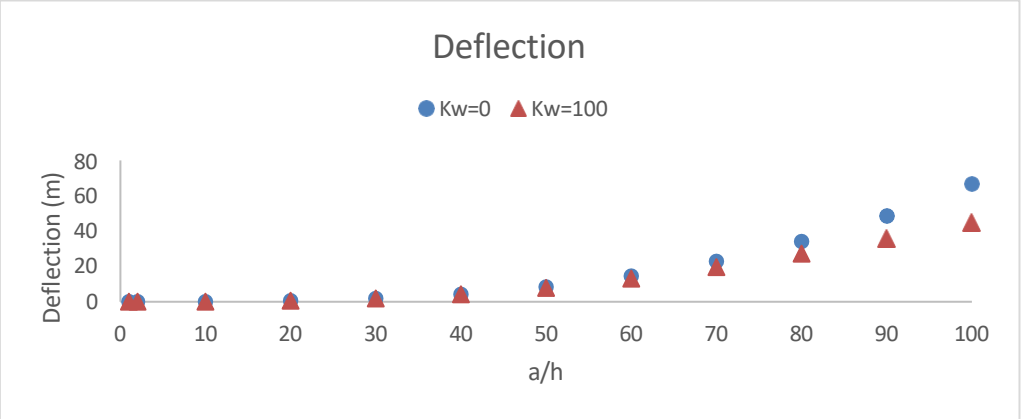


Figure 22 Deflection with varing a/h ratio.

Comparision of stress in different elastic foundation:

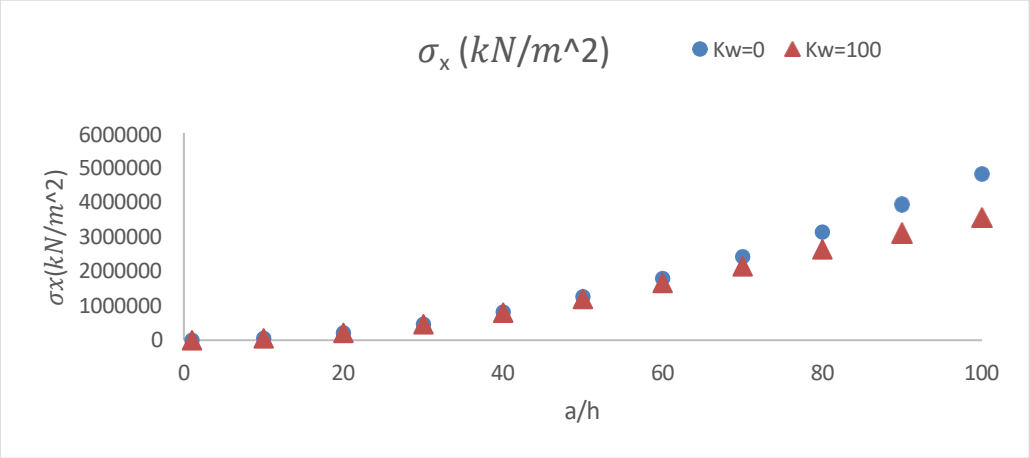


Figure 23 $\sigma_x$ with varing a/h ratio.

.

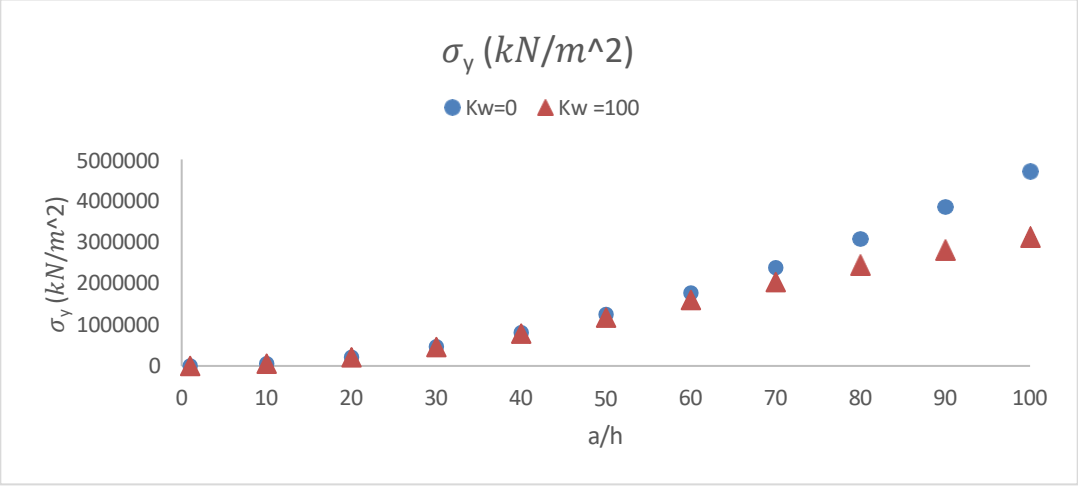


Figure 24 $\sigma_y$ with varing a/h ratio.

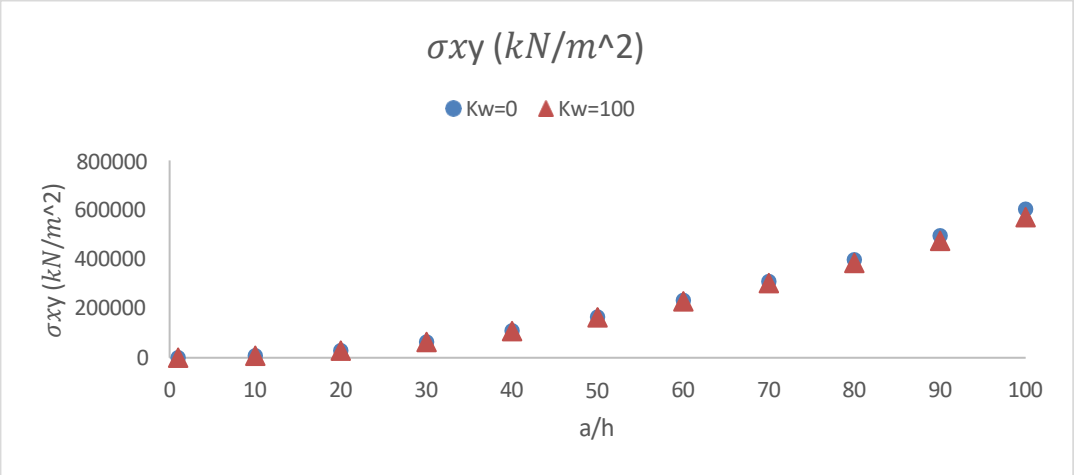


Figure 25 $\sigma_{xy}$ with varing a/h ratio.

The proportion of a plate's length to its height is a vital determinant of its structural behavior, specifically with respect to the levels of stress and deflection it experiences. When this ratio is low, the elastic foundation's effect on the plate is insignificant, with the thickness and material characteristics being the principal factors dictating its behavior. On the other hand, a high length to height ratio significantly impacts the plate's response, and the elastic foundation plays a significant role in this scenario, leading to a more complex analysis.

The elastic foundation's importance lies in the support it provides to the plate's load and its role in redistributing the load across the foundation. By offering additional resistance to the plate's deflection, the elastic foundation minimises the plate's stress and helps prevent failure. The impact of the elastic foundation on the plate, however, varies depending on factors such as the stiffness of the foundation, the loading conditions, and the plate's dimensions.

As the length to height ratio increases, the effect of the elastic foundation becomes more prominent, and the plate's response becomes more sensitive to any alterations in the foundation's stiffness. The foundation's stiffness impacts the distribution of stresses and the plate's deflection, which can lead to unpredictable behavior and failure if ignored in the analysis and design stages.

In conclusion, it is crucial to consider both the length to height ratio and the impact of the elastic foundation when analysing and designing plate structures. An understanding of these factors can assist engineers and designers in ensuring that the structure performs optimally and safely under various loading conditions. Accounting for these factors can lead to the

development of efficient and cost-effective designs that meet the desired performance and safety standards.

# Chapter 6
# CONCLUSION

The first-order shear deformation theory was employed to analyse the bending behaviour of cross-ply rectangular thick plates supported by an elastic foundation in this study. A Matlab code was developed based on this analysis, and a numerical example was used to validate the approach, with the results compared to the finite element method. The comparison demonstrated good agreement between the two methods, indicating the accuracy of the analysis.

The study further investigated the impact of the elastic foundation on the bending response of symmetrically laminated thick plates by solving several numerical examples. The results revealed that the foundation stiffness significantly affected the mid-plane deflections and stresses of the laminated plate. The impact of foundation stiffness decreased as the plate thickness ratio decreased, and when a/h reached 10, the deflection and shear stress distributions for both foundation stiffness values were almost identical. However, when a/h reached 100, there was a notable difference in the deflection and shear stress distributions for the two foundation stiffness values, emphasising the importance of considering the elastic foundation effect in thick plate bending analysis.

These findings provide useful insights for engineers and designers involved in the design and analysis of structures that incorporate thick plates. The developed Matlab code can be a valuable tool for accurately and efficiently assessing the bending behaviour of cross-ply rectangular thick plates supported by an elastic foundation. In summary, the study highlights the importance of considering the thickness ratio of the plate in relation to its length and width and emphasises the necessity of incorporating the effect of the elastic foundation in the analysis of thick plate bending behaviour.

# REFERENCES

[1] E. Reissner, "The Effect of Transverse Shear Deformation on the Bending of Elastic Plates", J. Appl. Mech., 12(1945), pp. 69–77.

[2] R. D. Mindlin, "Influence of Rotatory Inertia and Shear on Flexural Motions of Isotropic, Elastic Plates", J. Appl. Mech., 18(1951), pp. 31–38.

[3] E. Reissner, "On the Theory of Bending of Elastic Plates", J. Math. Phy., 23(1944), pp. 184–191.

[4] F. Norman, Jr. Knight, and Qi. Yunqian, "On a Consistent First-Order Shear-Deformation Theory for Laminated Plates", Composites Part B, 28B (1997), pp. 397–405.

[5] M. E. Fares, "Non-Linear Bending Analysis of Composite Laminated Plates Using a Refined First-Order Theory", Composite Structures, 46 (1999), pp. 257–266.

[6] K. Swaminathan, and D. Ragounadin, "Analytical Solutions Using a Higher-Order Refined Theory for the Static Analysis of Antisymmetric Angle-Ply Composite and Sandwich Plates", Composite Structures, 64(2004), pp. 405–417.

[7] A. J. M. Ferreira, C. M. C. Roque, and P. A. L. S. Martins, "Analysis of Composite Plates Using Higher-Order Shear Deformation Theory and a Finite Point Formulation Based on the Multiquadric Radial Basis Function Method", Composites Part B, 34(2003), pp. 627–636.

[8] A. M. Zenkour, "Exact Mixed-Classical Solutions for the Bending Analysis of Shear Deformable Rectangular Plates", Applied Mathematical Modelling, 27(2003), pp. 515–534.

[9] J. N. Reddy, "A Simple Higher Order Theory for Laminated Composite Plates", J. Appl. Mech., 51(1984), pp. 745–752.

[10] Nguyen, H.N. and Hong, T.T. and Van Vinh, P. and Quang, N.D. and Van Thom, D. (2019) A refined simple first-order shear deformation theory for static bending and free vibration analysis of advanced composite plates. Materials, 12 (15): 2385. ISSN 19961944